UNCLASSIFIED
SECURITY CLASSIFICATION OF THIS PAGE

REPORT DOCUMENTATION PAGE

DTIC FILE COPY

1a. REPORT SECURITY CLASSIFICATION: Unclassified	1b. RESTRICTIVE MARKINGS
2a. SECURITY CLASSIFICATION AUTHORITY	3. DISTRIBUTION / AVAILABILITY OF REPORT: Approved for public release; Distribution is unlimited (2)
2b.	
4. P AD-A203 071	5. MONITORING ORGANIZATION REPORT NUMBER(S)
6a. NAME OF PERFORMING ORGANIZATION: The University of Michigan Chemical Engineering	6b. OFFICE SYMBOL (If applicable)
6c. ADDRESS (City, State, and ZIP Code): 2130 H.H. Dow Building, Ann Arbor, Michigan 48109-2136	7a. NAME OF MONITORING ORGANIZATION: AFOSR/NC
	7b. ADDRESS (City, State, and ZIP Code): Building 410, Bolling AFB, D.C. 20332-6448
8a. NAME OF FUNDING / SPONSORING ORGANIZATION: AFOSR	8b. OFFICE SYMBOL (If applicable): NC
	9. PROCUREMENT INSTRUMENT IDENTIFICATION NUMBER: Grant/AFOSR-85-0027
8c. ADDRESS (City, State, and ZIP Code): Building 410, Bolling AFB, DC 20332-6448	10. SOURCE OF FUNDING NUMBERS

PROGRAM ELEMENT NO.	PROJECT NO.	TASK NO.	WORK UNIT ACCESSION NO.
61102F	2303	A1	

11. TITLE (Include Security Classification): Chemical and Electrochemical Properties of Potential Battery Systems in Room Temperature Molten Salts

12. PERSONAL AUTHOR(S): Francis M. Donahue, Leif Simonsen, Russell Moy, Sarah Borns

13a. TYPE OF REPORT	13b. TIME COVERED	14. DATE OF REPORT (Year, Month, Day)	15. PAGE COUNT
Final	FROM 84 TO 87	88, October 25	64

16. SUPPLEMENTARY NOTATION

17. COSATI CODES		
FIELD	GROUP	SUB-GROUP

18. SUBJECT TERMS (Continue on reverse if necessary and identify by block number): Electrochemistry, Molten Salt, Electrolyte, Aluminum, Zinc, Magnesium. (AW)

19. ABSTRACT (Continue on reverse if necessary and identify by block number)

Aluminum electrodes were studied in basic and acidic melts. Dissolution was possible in both environments, but deposition was possible only in acidic melts. Extensive studies in acidic melts indicated that the exchange current density was relatively low (even at 100°C, it was ≤1 mA/cm²) and that some passivation occurred at high current densities / ≥ 0.1 overpotentials. However, the dissolution behavior at moderate rates (≤ 10 mA/cm²) indicated relatively low polarization (sufficient for battery applications). Keywords:

20. DISTRIBUTION / AVAILABILITY OF ABSTRACT	21. ABSTRACT SECURITY CLASSIFICATION
☐ UNCLASSIFIED/UNLIMITED ☐ SAME AS RPT. ☐ DTIC USERS	UNCLASSIFIED

22a. NAME OF RESPONSIBLE INDIVIDUAL	22b. TELEPHONE (Include Area Code)	22c. OFFICE SYMBOL
Dr. John S. Wilkes	767-4960	NC

DD FORM 1473, 84 MAR — 83 APR edition may be used until exhausted. All other editions are obsolete.

SECURITY CLASSIFICATION OF THIS PAGE
UNCLASSIFIED

88 12 [illegible]

19. ABSTRACT CONTINUED

The $Al_2Cl_7^-$ anion was found to react with some basic, organic solvents (nitriles and amines) forming tetrahedral and octahedral aluminum complexes (ions and neutral molecules) with the organic base. The structure was determined from ^{27}Al nmr. The electrochemistry of the complexes formed with nitriles indicated that the dissolution process was significantly alterred (e.g., passivation was not observed) while deposition was not possible (due to the quantitative removal of $Al_2Cl_7^-$).

Corrosion of magnesium was essentially nil in basic and neutral melts (these melts were essentially free of impurities) indicating that the cation (1-methyl-3-ethylimidazolium) and tetrachloroaluminate anion were not electrochemically attacked by the metal. On the other hand, magnesium reacted with $Al_2Cl_7^-$ in acidic melts to form aluminum and a magnesium ionic species. Since ^{25}Mg nmr spectra could not be obtained at the concentration levels found in the melts, the structure of this magnesium species could not be determined. Magnesium was found to be stable in ternaries of acetonitrile and (initially acidic) binary melts.

Electrodissolution of zinc is more robust than aluminum (e.g., the exchange current densities in basic solutions are on the order of 0.1 mA/cm^2 at room temperature). Dissolution forms the anionic complex, $ZnCl_4^{2-}$, which was verified by the stoichiometry for the diffusivity measurement of Cl^-. Since ^{67}Zn nmr spectra could not be obtained at the concentration levels found in the melts, the structure could not be corroborated in this manner.

Aluminum electrodes were found to behave well in battery configurations with $FeCl_3$ and $CuCl_2$ 'positives'. Acidic, binary melts were completely reversible and were found to operate at current densities in excess of 15 mA/cm^2. Zinc electrodes were found to behave well in primary battery configurations with $FeCl_3$ and $CuCl_2$ 'positives'.

FINAL REPORT

Chemical and Electrochemical Properties of Potential Battery Systems in Room Temperature Molten Salts

Grant No. AFOSR-85-0027

Francis M. Donahue

Leif Simonsen
Russell Moy
Sarah Borns

Chemical Engineering Department
The University of Michigan
Ann Arbor, MI 48109-2136

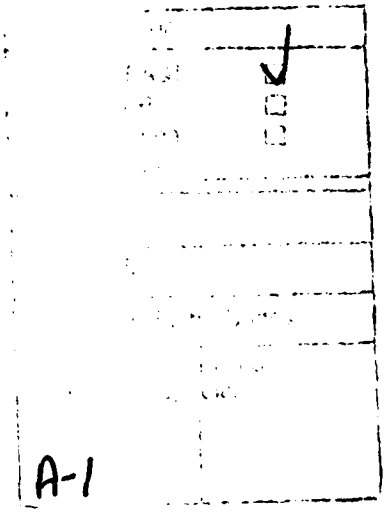

ABSTRACT

Aluminum electrodes were studied in basic and acidic melts. Dissolution was possible in both environments, but deposition was possible only in acidic melts. Extensive studies in acidic melts indicated that the exchange current density was relatively low (even at ≈ 100°C, it was ≈ 1 mA/cm^2) and that some passivation occurred at high current densities / overpotentials. However, the dissolution behavior at moderate rates (≤ 10 mA/cm^2) indicated relatively low polarization (sufficient for battery applications).

The $Al_2Cl_7^-$ anion was found to react with some basic, organic solvents (nitriles and amines) forming tetrahedral and octahedral aluminum complexes (ions and neutral molecules) with the organic base. The structure was determined from ^{27}Al nmr. The electrochemistry of the complexes formed with nitriles indicated that the dissolution process was significantly alterred (e.g., passivation was not observed) while deposition was not possible (due to the quantitative removal of $Al_2Cl_7^-$).

Corrosion of magnesium was essentially nil in basic and neutral melts (these melts were essentially free of impurities) indicating that the cation (1-methyl-3-ethylimidazolium) and tetrachloroaluminate anion were not electrochemically attacked by the metal. On the other hand, magnesium reacted with $Al_2Cl_7^-$ in acidic melts to form aluminum and a magnesium ionic species. Since ^{25}Mg nmr spectra could not be obtained at the concentration levels found in the melts, the structure of this magnesium species could not be determined. Magnesium was found to be stable in ternaries of acetonitrile and (initially acidic) binary melts.

Electrodissolution of zinc is more robust than aluminum (e.g., the exchange current densities in basic solutions are on the order of 0.1 mA/cm^2 at room temperature). Dissolution forms the anionic complex, $ZnCl_4^{2-}$, which was verified by the stoichiometry for the diffusivity measurement of Cl^-. Since ^{67}Zn nmr spectra could not be obtained at the concentration levels found in the melts, the structure could not be corroborated in this manner.

Aluminum electrodes were found to behave well in battery configurations with $FeCl_3$ and $CuCl_2$ 'positives'. Acidic, binary melts were completely reversible and were found to operate at current densities in excess of 15 mA/cm^2. Zinc electrodes were found to behave well in primary battery configurations with $FeCl_3$ and $CuCl_2$ 'positives'.

TABLE OF CONTENTS

INTRODUCTION

This report has been divided into six Sections which represent major thrust areas in the research. The first section addresses physicochemical measurements - particularly an evaluation of shear rate-dependent viscosity measurements. The second and third Sections (as well as the previously-reported Electrochimica Acta, Vol. 33, No. 5, pp 721-724, 1988) discuss the dissolution behavior of aluminum in binary and ternary solutions of the low-temperature molten salts with particular emphasis on the potential problem of passivation of battery negatives. Sections 4 and 5 present results for the dissolution of zinc and magnesium, respectively; two materials which hold some promise as negatives in primary and/or reserve applications. The final part, Section 6, reports on some battery configurations for binary and ternary solutions of the molten salts with particular emphasis on secondary (rechargeable) batteries.

Section 1. Viscosity Measurements of Low Temperature Molten Salts

Low temperature molten salts are a new class of electrolytes for battery applications (e.g., see Ref. 1). Viscosity measurements of low temperature molten salts based on mixtures of aluminum or copper halide and alkylpyridinium or dialkylimidazolium halide have been reported (1-5). They have shown strong dependences of viscosity with changes in composition in basic (i.e., organic-rich) melts (1, 2, 4, 5). Further, "gaps" in the liquidus lines, i.e., regions where fusion does not occur - only a glass transition at very low temperatures, have been shown for binary melts containing 1-methyl-3-ethylimidazolium chloride (MEIC) (1) and bromide (2) as the organic salt. Finally, measurements of chemical shifts for proton and carbon nuclear magnetic resonance spectra of basic MEIC-$AlCl_3$ melts have been explained in terms of oligomeric structures (6, 7). All of these measurements used viscometers based on variations of Cannon-Fenske devices (1-3, 5) or the falling ball method (4). These methods do not provide shear stress - shear rate data, which could be used to determine whether the melts behave like non-Newtonian fluids. This paper reports viscosity measurements of MEIC-$AlCl_3$ binary melts using a plate and cone viscometer (in order to obtain shear stress - shear rate data) and compares the viscosities measured using this technique with those of previous investigators.

The organic salt was synthesized and purified similarly to the method of Wilkes and coworkers (8). Aluminum chloride (Fluka puriss.) was sublimed from a mixture of NaCl and aluminum wire in an evacuated vessel at 170°C onto a 'cold finger' cooled by an external flow of air. The viscometer was a Brookfield Model LVTD Digital Viscometer with CP-40, CP-42, and CP-52 cones. Temperature control was maintained by recirculating water through an insulated tube from a Lauda Model TK-30 constant temperature bath to the jacketed sample holder of the viscometer. The viscosity measurements were carried out in a Vacuum Atmospheres Company dry box equipped with a "Dri Train" having oxygen removal capabilities. The dry box atmosphere was a mixture of purified helium and nitrogen. A summary of the experiments carried out is shown in Table 1.

In order to determine whether the melts exhibited Newtonian or non-Newtonian behavior, the shear stress - shear rate data were analyzed according to the power law equation (Ostwald-de Waele Model) (9), i.e.,

$$\tau = m \gamma^n \qquad [1]$$

where τ is the shear stress, m is the consistency, γ is the shear rate, and n is the flow index (n = 1 for Newtonian fluids and n < 1 for pseudoplastic fluids). Values of the consistency and flow index were obtained from log-log plots of the shear stress vs. the shear rate. The viscosity, μ, was computed from

$$\mu = m \gamma^{n-1} \qquad [2].$$

With the exceptions of the data from melts with a nominal $AlCl_3$ mol fraction, N, of 0.35 at $30 \geq T/^{\circ}C \geq 10$ and for N = 0.40 at all temperatures indicated, the flow index was 1.00 +/- 0.02 - indicating Newtonian behavior.

The experiments which seemed to indicate non-Newtonian behavior were analyzed in order to compute the viscosity - shear rate relationship. The flow index was found to be equal to or greater than 0.90*, but always less than unity - indicating a slight dependence of the viscosity on the shear rate and slight pseudoplastic behavior. It is of interest that the melts which show this behavior are found in the vicinity of the liquidus "gap" mentioned above. Figure 1 shows some of the data which exhibit this shear-thinning behavior.

Even the experiments which had flow indices less than unity (i.e., non-Newtonian behavior) exhibited linear dependencies of shear stress on shear rate for all practical purposes. In the absence of stronger evidence of non-Newtonian behavior, the viscosities for these melts (as well as those for which Newtonian behavior was observed) were computed from the linear shear stress - shear rate data. Figure 2 shows the computed values of viscosities from these experiments (symbols) while the curves show a correlation for viscosity developed by Fannin and coworkers for these binary melts based on their measurements (1). The agreement between these data and the correlation indicates that the viscosity can be conveniently obtained for these (and similar) melts by either of the methods employed in the respective studies.

Unlike some studies on similar molten salts (1,2), the viscosity data obtained in this study did provide an Arrhenius relationship over the entire temperature range. The

* A Student t-test of the data for these melts indicated that the slope of the log shear stress - log shear rate data were statistically different than 1.00 at the 90% level of significance.

computed activation energies are shown in Table 2. These values are very close to those computed by Fannin at 30°C (1), significantly larger than those reported for molten $HgCl_2$ (10) and molten pyridinium salts (11, 12), similar to (but less than) those for CuCl-MEIC binaries in basic melts (5), smaller than those for acidic CuCl-MEIC binaries where the viscosity rises steeply with increasing CuCl mol fraction (5), and approximately the same as those calculated by Carpio and coworkers for acidic alkylpyridinium chloride-$AlCl_3$ binaries (3). Although providing no quantitative information concerning melt structure, the magnitude of the activation energies, particularly in the more basic melts, indicates strong interactions among the components (1) - exceeding those of typical physical processes.

Symbols

m = consistency (units dependent upon value of flow index)
n = flow index (dimensionless)
γ = shear rate (s^{-1})
μ = viscosity (cP; mPa s)
τ = shear stress (dyne cm^{-2})

References

1. A. A. Fannin, D. A. Floreani, L. A. King, J. S. Landers, B. J. Piersma, D. J. Stech, R. L. Vaughn, J. S. Wilkes, and J. L. Williams. **J. Phys. Chem., 88**, 2614 (1984).

2. J. R. Sanders, E. H. Ward, and C. L. Hussey. **J. Electrochem. Soc., 133**, 325 (1986).

3. R. Carpio, L. A. King, R. E. Lindstrom, J. C Nardi, and C. L. Hussey. **ibid., 126**, (1979).

4. C. Nanjundiah, K. Shimizu, and R. A. Osteryoung. **ibid., 129**, 2474 (1982).

5. S. A. Bolkan and J. T. Yoke. **J. Chem. Eng. Data, 31**, 194 (1986).

6. A. A. Fannin, L. A. King, J. A. Leviskey, and J. S. Wilkes. **J. Phys. Chem., 88**, 2609 (1984).

7. J. S. Wilkes, C. L. Hussey, and J. R. Sanders. **Polyhedron, 5**, 1567 (1986).

8. J. S. Wilkes, J. A. Leviskey, R. A. Wilson, and C. L. Hussey. **Inorg. Chem., 21**, 1263 (1982).

9. R. B. Bird, W. E. Stewart, and E. N. Lightfoot. **Transport Phenomena**. Wiley, New York, 1960. pp. 10-14.

10. G. J. Janz and J. D. E. McIntyre. **J. Electrochem. Soc., 109**, 842 (1962).

11. D. S. Newman, R. T. Tillack, D. P. Morgan, and W-C. Wan. **ibid., 124**, 856 (1977).

12. D. S. Newman and R. M. Stevens. **ibid., 131**, 1275 (1984).

Table 1. Summary of Viscosity Data

Nominal $AlCl_3$ Mol Fraction	Temperature Range/°C*	Number of Data Pairs**
0.31	20-40	5- 7
0.35	10-35	7-11
0.40	10-35	8-10
0.45	0-25	4- 5
0.64	10-35	3- 4

* in 5°C increments;
** at each temperature.

Table 2. Computed Activation Energies (kcal/mol).

Nominal $AlCl_3$ Mol Fraction	Activation Energy
0.31	12.4
0.35	10.9
0.40	8.4
0.45	6.9
0.64	5.3

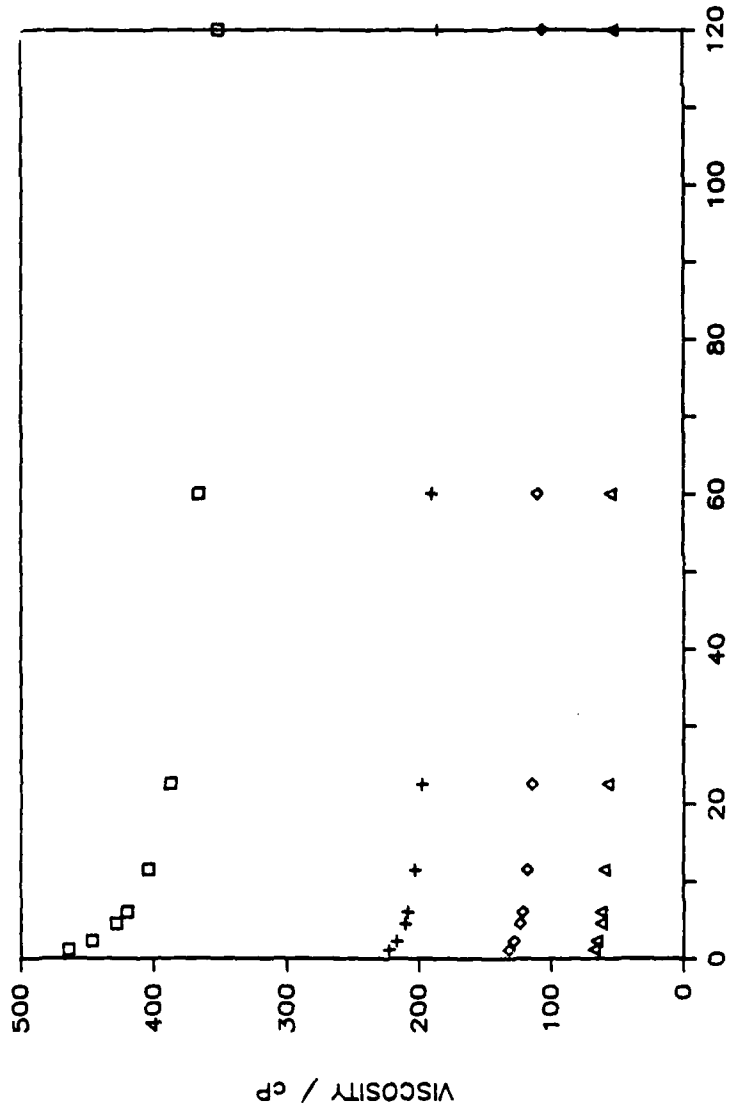

Figure 1. Viscosity - Shear Rate behavior of melts with flow indices less than unity.
N = 0.35: squares, 10°C; crosses, 20°C;
N = 0.40: diamonds, 15°C; triangles, 30°C.

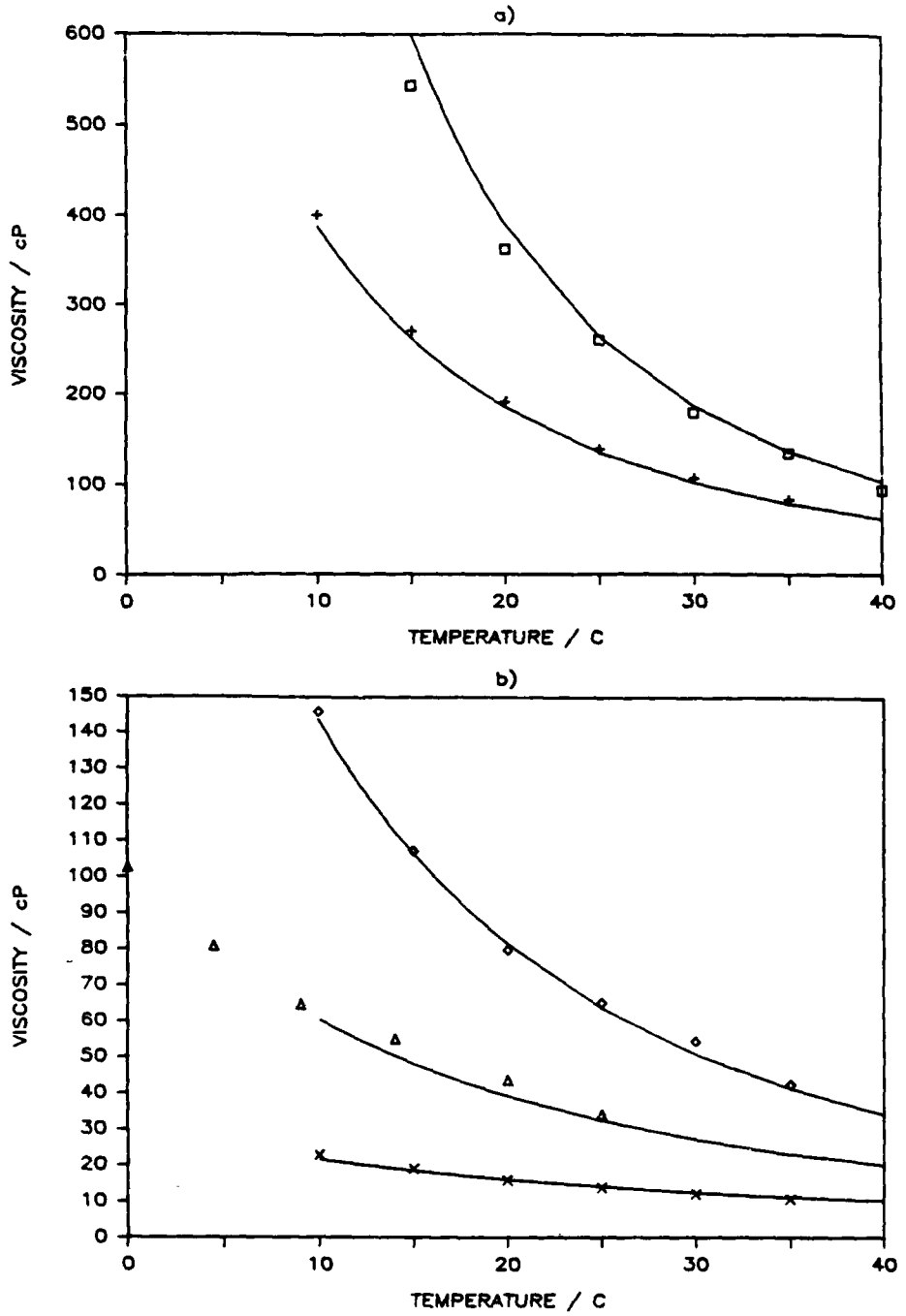

Figure 2. Viscosity - Temperature behavior of melts.
a) squares, N = 0.31; crosses, N = 0.35;
b) diamonds, N = 0.40; triangles, N = 0.45;
x's, N = 0.64;

Section 2. Anodic Passivity of Aluminum in Acidic Chloroaluminate Molten Salts

Aluminum electrochemistry has been studied extensively in acidic ($AlCl_3$-rich) (1-24) and basic (RCl-rich) (1,13,14,25-31) chloroaluminate molten salts, having both inorganic (1-10,14,19,20,25,31) and organic cations (2,11-13,15-18,21-24). Al(III) exists as complex anions in these electrolytes; in acidic electrolytes, the anionic species are $Al_2Cl_7^-$ and $AlCl_4^-$. Tremillion and Letesse (1) have shown that aluminum oxidation in acidic chloroaluminate electrolytes proceeds according to:

$$Al + 7\ AlCl_4^- = 4\ Al_2Cl_7^- + 3\ e^- \qquad [1]$$

Cyclic voltammetry of inert electrodes has been used to verify the electrochemical oxidation of thin aluminum deposits in these electrolytes (9,11,13,17,23,24). MacArthur (21,22) integrated the cathodic and anodic peak areas of molybdenum electrode CVs and found that the efficiency of the dissolution reaction was unity under certain conditions. Cyclic voltammograms of solid aluminum electrodes were used to confirm the oxidation of bulk aluminum in acidic imidazolium chloroaluminate electrolytes (13,21,22).

Current reversal chronopotentiometry has been used to characterize the dissolution of aluminum thin films cathodically deposited on inert substrates (8,11,17,23,24). Anodic transition times were shorter than expected for the depletion of aluminum. This inefficiency was believed to be due to aluminum corrosion in the electrolyte.

Delimarskii (4) and Storozhenko (32) studied the oxidation of solid aluminum electrodes and gravimetrically determined that the current efficiency exceeded 100 percent. Protonic impurities in (5) may be responsible for a parallel corrosion reaction. Storozhenko (32) accounted for open circuit aluminum corrosion and concluded that soluble subvalent aluminum species were formed at 300 C.

Mamantov (7) obtained repeatable chronopotentiometric transitions when aluminum anodes were polarized galvanostatically at temperatures up to 200 C. These transitions were characteristic of anodic passivity, and Mamantov believed that as reaction [1] proceeded, there was a sufficient increase in the interfacial acidity to precipitate aluminum chloride on the electrode. Anodic passivation of aluminum was also reported by King (2) for aluminum chloride electrolytes containing sodium chloride or ethylpyridinium bromide, and by Piontelli (33) in sodium chloroaluminate molten salts at 200 C.

Above 200 C the chronopotentiometric transition time may be too long to detect (7,32). Del Duca (5) did not report aluminum passivation, although her data showed an

increase in the anodic exchange current density above 213 C in both neutral and acidic chloroaluminate melts. The exchange current density appeared to be independent of the cation or melt acidity for neutral or moderately acidic melts (Del Duca).

Holleck and Giner (3,6) and Eckeret and Fischer (20) found that even under forced convection aluminum electrodes became anodically passivated. Holleck and Giner found that the passive current increased with rotation rate of disk electrodes in accordance with Levich (34), and concluded that the dissolution rate of aluminum chloride, precipitated on the electrode, established the passive current. Eckeret and Fischer (20) found that the passive current was independent of mass transfer, but concurred on the explanation of the passivity. The insensitivity of the aluminum dissolution rate was on mass transfer was also observed by Del Duca (5)

Takahashi (19) did not observe anodic passivation of the aluminum RDE. However, he presented only limited data obtained with a 200 mV/sec linear potential ramp. Under these conditions, it is possible that insufficient charge was passed to form a complete passive layer. Passivation was not reported in the cyclic voltammetry data (9,11,13,17,23,24) because the current decay due to passivation was masked by the increasing diffusion layer thickness. Passivation may also be partially responsible for the "short" anodic transition times obtained with reverse current chronopotentiometry (8,11,17,23).

In the present work, we used an imidazolium chloride-aluminum chloride molten salt as a model system to study the mechanism of aluminum electrodissolution in acidic chloroaluminate electrolytes. An aluminum rotating cylinder electrode was selected as the test electrode because its hydrodynamics are relatively insensitive to changes in surface roughness that may occur during metal deposition and dissolution, and reliable correlations have been developed to describe the mass transfer at the RCE interface (35,36).

Experimental

1-Methyl-3-ethylimidazolium chloride (MEIC) was prepared according to Wilkes (37) except that the reaction temperature was 60 C, and the synthesis was conducted in the dark. Aluminum chloride (Fluka, puriss.) was purified at 190 C by vacuum sublimation from $AlCl_3$/NaCl/Al mixtures. The molten salt was prepared by the slow addition of MEIC to the aluminum chloride. Some of the electrolytes were conditioned by exhaustive electrolysis ($i < 1$ mA cm^{-2}) between two high purity (m5N) aluminum electrodes to remove trace impurities. Impurities were detected as an absorbance at 325 and 290 nm with UV-visible spectroscopy. The additional treatment removed the straw color from the electrolyte but did not effect the experimental results described below.

Working and counter electrodes, fabricated from high purity (m5N) aluminum rod (Johnson Matthey), were cleaned ultrasonically in acetone and methanol baths and dried under vacuo before use. A Pine Instruments Company Model MSR rotator was used to control the working electrode. Potentials are reported with respect to a reference electrode consisting of an aluminum plated platinum wire in an $X_{AlCl3} = 0.505$ melt and was separated from the working electrolyte by an ultra fine porosity glass frit.

The cell was thermostated in a sand bath (Thermolyne, Model 17600). Most of the experiments were conducted at 40 C, although similar results were obtained between 20 and 30 C. All experiments were conducted in a helium/argon filled dry box with continuous moisture and oxygen removal.

The test cell was controlled electronically with a Princeton Applied Research Model 273-97 potentiostat. This potentiostat has the capability to continuously correct for the internal resistance of the electrochemical cell by periodic current interruption. A maximum interruption frequency was selected, but in all cases the duty cycle for the cell was greater than 99 %. Data were saved digitally with an IBM-XT computer that was connected to the potentiostat through an IEEE-488 interface bus.

Results and Discussion

Figure 1 is a cyclic voltammogram of an aluminum rotating cylinder electrode in an acidic MEIC/$AlCl_3$ molten salt. The anodic current peak at +500 mV and potential-independent passive current on the return scan indicate that a film was formed electrochemically on the working electrode. The current response expected for this system under diffusion control is superimposed for comparison. When cyclic voltammograms were obtained at ambient temperature (without the sand bath), a black film could be seen forming on the electrode at the Flade potential. This film appeared stable at the passive potentials, and did not dissolve until about 400 mV on the return scan. Anodic formation of dark films on aluminum have also been reported by Delimarskii et al (5), Mamantov et al (7), and Osteryoung (8),

We were unable to obtain a reliable steady state current response for the potentiostatic polarization of the aluminum RCE. Traditional electrochemical data such as Tafel slopes, exchange current densities and diffusion limited currents cannot be reliably measured in these systems. Similar problems are encountered with transient electrochemical techniques, such as cyclic voltammetry and chronopotentiometry. These complications are responsible for the lack of kinetic data for reaction [1] in the literature.

We developed an open circuit potential relaxation technique that was useful for the characterization of aluminum oxidation in chloroaluminate molten salts. Here, a

potential anodic to the Flade potential was applied to the working electrode in order to generate the passive film. Then, the open circuit potential of the working electrode was recorded as a function of time. If the electrochemically generated films decompose on open circuit, the potential decay will correspond to the chemical reduction of the film. Heterogeneous films having multiple valencies are expected to have a stepwise potential decay (38,39).

Three acidic electrolytes were used to evaluate the influence of the concentration of $AlCl_4^-$ and $Al_2Cl_7^-$ on the electrode processes. The electrolytes and their physical properties are listed on Table 1. These electrolytes were selected because of their differing tetrachloroaluminate and heptachloroaluminate concentrations.

Figure 2 shows the initial current of a well cycled working electrode in response to a potentiostatic step of 700 mV. The current passes through a peak and shoulder after about 300 ms. Two distinct current peaks can be seen when a fresh electrode was used. This behavior was unexpected for simple metal dissolution reactions where the current would be essentially constant on this time scale.

Electrochemical nucleation of passive films produces a current peak in response to an applied potential step. Individual sites behave as an array of microelectrodes, with the current increasing as the nucleation of new sites proceeds. Planar electrode behavior is observed when intercrystal collisions occur. The formation of an insulating film on the electrode masks areas of the electrode from reacting further, and the current density decreases (40).

For aluminum dissolution in chloroaluminate molten salts, the peak current density and the eventual passive current density were very dependent on the roughness of the electrode. Both the peak current and passive current were found to increase with subsequent experiments. Visual inspection of the electrode after a series of runs indicates that the aluminum RCE becomes roughened during these experiments. The current peak and passive current were also increased when the electrode was roughened by abrasion of the RCE with SiC paper, or by the dendritic deposition of aluminum on the RCE substrate.

Figure 3 shows the passive current density as a function of run number for experiments that alternated between 500 and 800 RPM. There was only a slight increase in the current density at the higher rotation rate. The dashed line in Figure 3 shows the expected increase in current for the 800 RPM data if mass transfer were rate controlling. Faster rotation rates were not used in this comparison because the mechanical integrity of the film was compromised at higher speeds. This mechanical disruption can be observed visually, and produces an erratic current increase. Slow rotation rates were not used as

mass transfer correlations for the RCE are only valid above Reynolds numbers of 112 (35,36).

When potentials that were less anodic than the Flade potential were applied to the aluminum RCE, there was no evidence of a nucleation current peak, although the current response drifted during the polarization (Figure 4). Slow cyclic voltammograms of the RCE taken in the "active" region show a hysteresis, with the current maximum on the return scan (Figure 5). This is the current response expected for a cyclic voltammogram of a nucleation process if the potential is reversed before intercrystal collisions occur (41).

When the cell was placed on open circuit, the potential of the passivated RCE decayed through two arrests at approximately 360 and 330 mV. These potentials were independent of the electrolyte compositions tested. Figure 6 shows the repeatability of the potential arrests for subsequent experiments, and in different composition electrolytes. This two step potential relaxation was also reported by King et al (2) for aluminum anodes in ethylpyridinium bromo-chloroaluminate. The potential relaxation following anodic polarization in the "active" region did not produce these arrests (Figure 7). Instead, the potential decayed smoothly in one to two seconds as would be expected for the relaxation of interfacial concentration gradients.

Traditional chronopotentiometric analysis was used to determine the transition time of the arrests (42). Over the course of the experiments, the transition time of the 360 mV arrest was unchanged while the 330 mV arrest increased with subsequent experiments. Electrode rotation rate had no effect on the duration of the arrests (Figure 8). The increased electrode roughness was clearly responsible for the increasing transition time for the 330 mV plateau. The duration of the arrests was also affected by the time of the applied potential step, and surface variations that occur in the machining of the electrodes. However, electrode roughness was the dominant factor influencing the duration of the arrests and the passive current density. Mechanical, chemical, and electrochemical polishing techniques were tested in attempt to produce a repeatable starting surface. Unfortunately these procedures introduced impurities into the electrode that could be detected by ESCA analysis.

Conclusions

The rate of aluminum oxidation in acidic chloroaluminate molten salts was impaired by the formation of a passive film on the anode. Significant passive currents were measured, indicating that the film was thin. The insensitivity of the passive current to potential on the return scan of the cyclic voltammogram (Figure 1) shows that the

thickness of the film was constant on this time scale and is independent of the applied potential. However, continuous generation of the film was demonstrated by the presence of the anodic current. Therefore, a dynamic equilibrium thickness of the film was maintained by the continuous formation and dissolution of the film on polarized electrodes. The insensitivity of the passive current on the rotation rate of the RCE indicates that decomposition of the passive film on polarized electrodes was not mass transfer controlled. The open circuit decomposition of this film occurred in two repeatable steps, and was also independent of interfacial mass transfer. These features would not be expected for films consisting of species that were soluble in the electrolyte such as aluminum chloride. The decomposition of the film appears to be under kinetic control, rather than mass transfer control.

We believe that the film consists of reaction intermediates that were generated during the oxidation of aluminum. The passive current was established by the simultaneous generation of the film and kinetic decomposition of the film. On open circuit, solution or surface species reduce these intermediates, to produce the potential arrests described above.

The passive rate limitation can be circumvented by amalgamation of the electrode (43), or by the addition of certain cosolvents to the electrolyte(44). The mercury film seems to eliminate sites for the film formation and may alter the intermediates produced during the reaction. Certain cosolvents can significantly alter the nature of the ions in chloroaluminate electrolytes, and undoubtedly offer an alternate reaction pathway.

References

1. Tremillon, B., and G. Letisse, *J. Electroanal. Chem.*, **17**, 371-386, (1968).

2. King, L.A., A.D. Brown, F.H. Frayer, "Proceedings of the 1968 OAR Research Applications Conference", Vol. 1, Institute for Defense Analyses Rep. OAR-68-001, AD-666800, (1968).

3. Giner, J., and G.L. Holleck, NASA CR 1541, (1968).

4. Delimarskii, Yu.K., V.F. Makogon, and A.Ya., Zhigailo, *Elektrokhimiya*, **5**, 108-110, (1969).

5. Del Duca, B.S., *J. Electrochem Soc.*, **118**, 405-411, (1971).

6. Holleck , G.L., and J. Giner, *J. Electrochem. Soc.*,**119**, 1161-1166, (1972).

7. Gilbert, B., D.L. Brotherton, and G. Mamantov, *J. Electrochem. Soc.*, **121**, 773-776, (1974).

8. Gale, R.J., and R.A. Osteryoung, *J. Electrochem. Soc.*, **121**, 983-987, (1974).

9. Rolland, P., and G. Mamantov., *J. Electrochem. Soc.*, **123**, 1299-1303, (1976).

10. Gorodyskii, A.V., Yu.K. Delimarskii, and V.A. Bagrii, *Ukr. Khim. Zh.*, **45**, 579-582, (1979).

11. Robinson, J., and R.A. Osteryoung, *J. Electrochem. Soc.*, **127**, 122-128, (1980).

12. Welch, B.J., and R.A. Osteryoung, *J. Electroanal. Chem.*, **118**, 455-466, (1981).

13. Piersma, B.J., and J.S. Wilkes, Frank J. Seiler Research Laboratory Technical Report FJSRL-TR-82-0004, (1982).

14. Bagrii, V.A., *Ukr. Khim. Zh.*, **48**, 1107-1108, (1982).

15. Wilkes, J.S., and J.J. Auborn, Abstract 242, Electrochemical Society Fall Meeting, (1983).

16. Auborn, J.J., and Y.L. Schregenberger, Abstract A4-13, International Society of Electrochemistry 35th Meeting, (1984).

17. Qin, Q-X., and M. Skyllas-Kazacos, J. *Electroanal. Chem.*, **168**, 193-206, (1984).

18. Auborn, J.J., and Y.L. Barberio, *J. Electrochem. Soc.*, **132**, 598-601, (1985).

19. Takahashi, S., and N. Koura, *J. Electroanal. Chem.*, **188**, 245-255, (1985).

20. Eckert, J., and F. Fischer, *Z. Phys. Chemie*, **266**, 572-578, (1985).

21. MacArthur, D.M., and R.M. Bendert, "The Aluminum Electrode in 1-Ethyl-3-Methylimidazolium Chloride/Aluminum Trichloride Liquid Electrolytes" General Motors Research Report GMR-5116, (1985).

22. MacArthur, D.M., and R.M. Bendert, Abstract 403, Electrochemical Society Spring Meeting, (1986).

23. Lai, P.K., and M. Skyllas-Kazacos, *Electrochemica Acta*, **32**, 1443-1449, (1987).

24. Chryssoulakis, Y., J-C. Poignet, and G. Manoli, *J. Applied Electrochem.*, **17**, 857-867, (1987).

25. Carpio, R.A., and L.A. King, *J. Electrochem. Soc.*, **128**, 1510-1517, (1981)

26. Fellner, P., Z. Lubyova, and M. Gabco, *Chem. Zvesti*, **37**, 617-622, (1983).

27. Gabco, M., P. Fellner and Z. Lubyova, *Electrochimica Acta*, **29**, 397-401, (1984).

28. Bjorgum, A., A. Sterten, J. Thonstad, R. Tunold, and R. Ødegard, *Electrochimica Acta*, **29**, 975-977, (1984).

30. Bouteillon, J., and A. Marguier, *Surface Technology*, **22**, 205-217, (1984).

31. Hauksson, T., and F.R. Foulkes, *Can. J. Chem. Eng.*, **63**, 237-243, (1985).

32. Storozhenko, V.N., *Elektrokhimiya*, **8**, 973-976, (1972).

33. Piontelli, R., G. Sternheim, and M. Francini, *J. Chem. Phys.*, **24**, 1113-1114, (1956).

34. Levich, V.G., **Physiochemical Hydrodynamics**, pp. 286-293, Prentice Hall, Inc., Englewood Cliffs, NJ, (1962).

35. Eisenberg, M., C.W. Tobias, and C.R. Wilke, *Chemical Engineering Progress Symposium Series*, **16**, 1-16, (1955).

36. Newman, J.S., **Electrochemical Systems**, pp. 324-326, Prentice Hall, Inc., Englewood Cliffs, NJ, (1973).

37. Wilkes, J.S., J.A. Levisky, R.A. Wilson, and C.L. Hussey, *Inorg. Chem.*,**21**, 1263-1264, (1982).

38. Nardi, J.C., *J. Electrochem. Soc.*, **132**, 1787-1791,(1985).

39. Haung, C-K., A. Anani, S. Crouch-Baker, and R.A. Huggins, Abstract 96, Electrochemical Society Fall Meeting, (1986).

40. Astley, D.J., J.A. Harrision, and H.R. Thirsk, *Trans. Far. Soc.*, **64**, 192-201, (1968).

41. Fletcher, S., C.S. Halliday, D. Gates, M. Westcott, T. Lwin, and G. Nelson, *J. Electroanal. Chem.*, **159**, 267-285, (1983).

42. Plambeck, J.A., **Electroanalytical Chemistry--Basic Principles and Applications**, pp. 359-361, John Wiley and Sons, New York, (1982).

43. Moy, R., and F.M. Donahue, *Electrochimica Acta*, **33**, 721-724, (1988).

44. Donahue, F.M., L.R. Simonsen, and R. Moy, Unpublished results.

X_{AlCl3}	ρ/g cm^{-3}	η/cP	κ/mmho cm^{-1}	$[AlCl_4^-]$/M	$[Al_2Cl_7^-]$/M	$\varphi_{0,Al}$/mV
0.520	1.292	11.8	30.0	4.07	0.37	66
0.570	1.318	11.1	26.0	2.75	1.33	110
0.635	1.356	10.1	21.7	0.93	2.65	204

Table 1. Properties of the electrolytes studied (40 C).

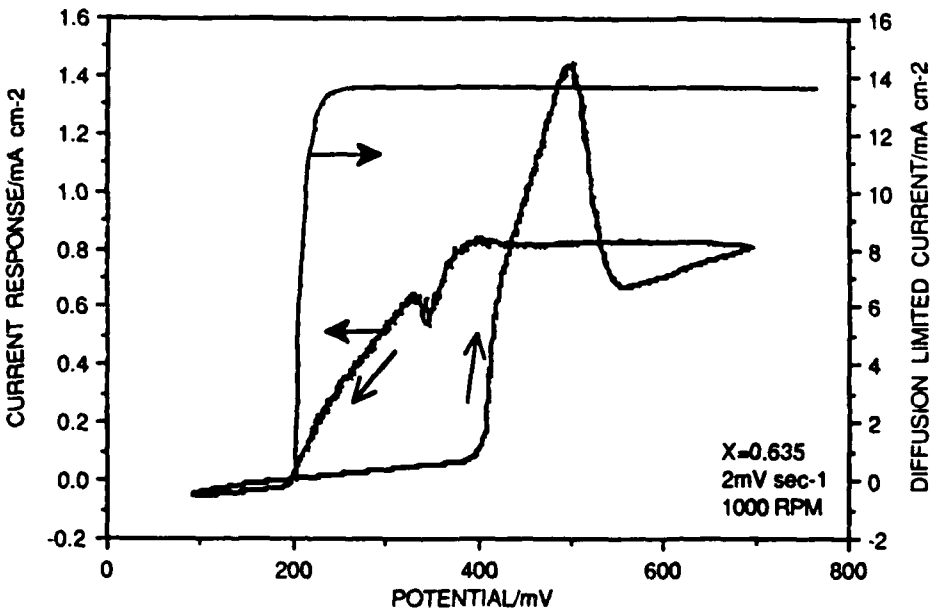

Figure 1. Cyclic voltammogram of aluminum rotating cylinder electrode in acidic MEIC/$AlCl_3$ molten salt.

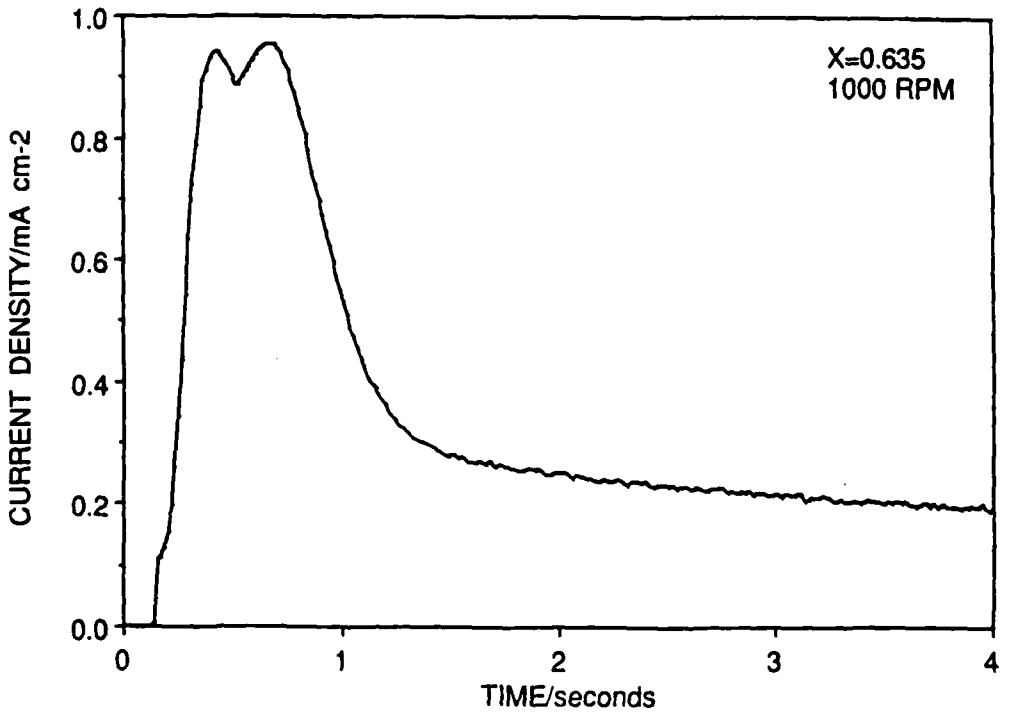

Figure 2. Initial current resopnse of an aluminum rotating cylinder electrode during a 700 mV potentiostatic step.

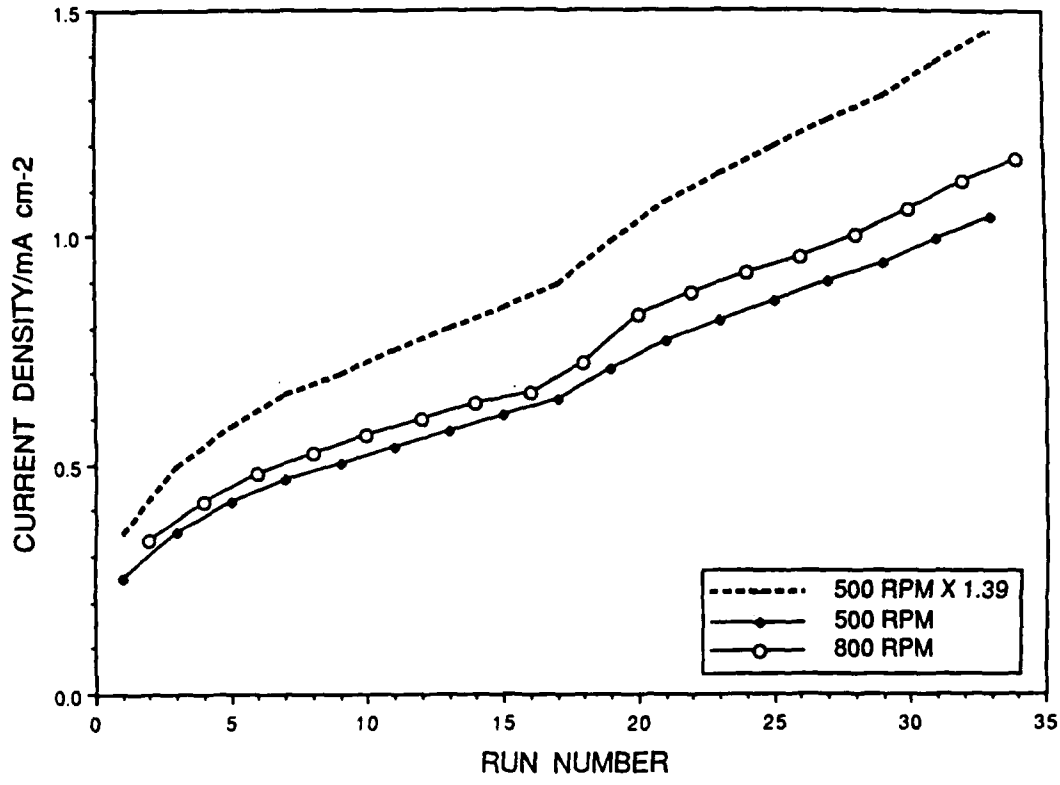

Figure 3. Increase in the passive current with subsequent experiments. The working electrode was on open circuit for 18 minutes between the experiments. The dashed line is the expected increase in the current response when the rotation rate is increased from 500 to 800 RPM if mass transfer were controlling.

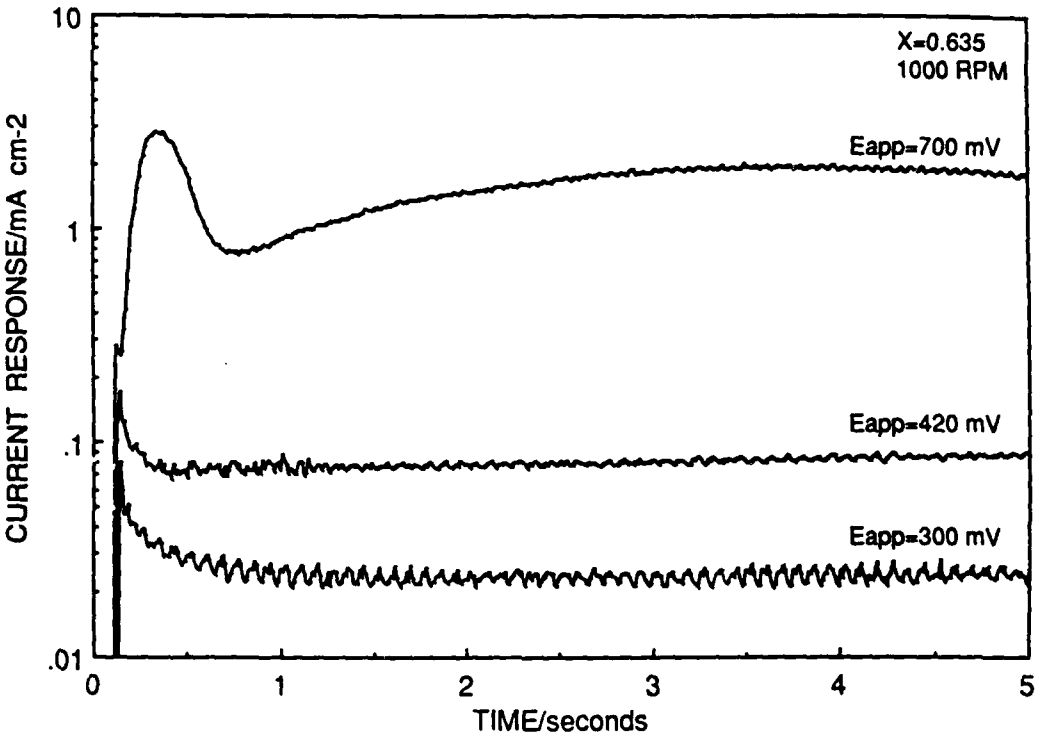

Figure 4. Initial current response of aluminum rotating cylinder electrode during 700, 420, and 300 mV potentiostatic steps. The passive potential in Figure 1 is 500 mV.

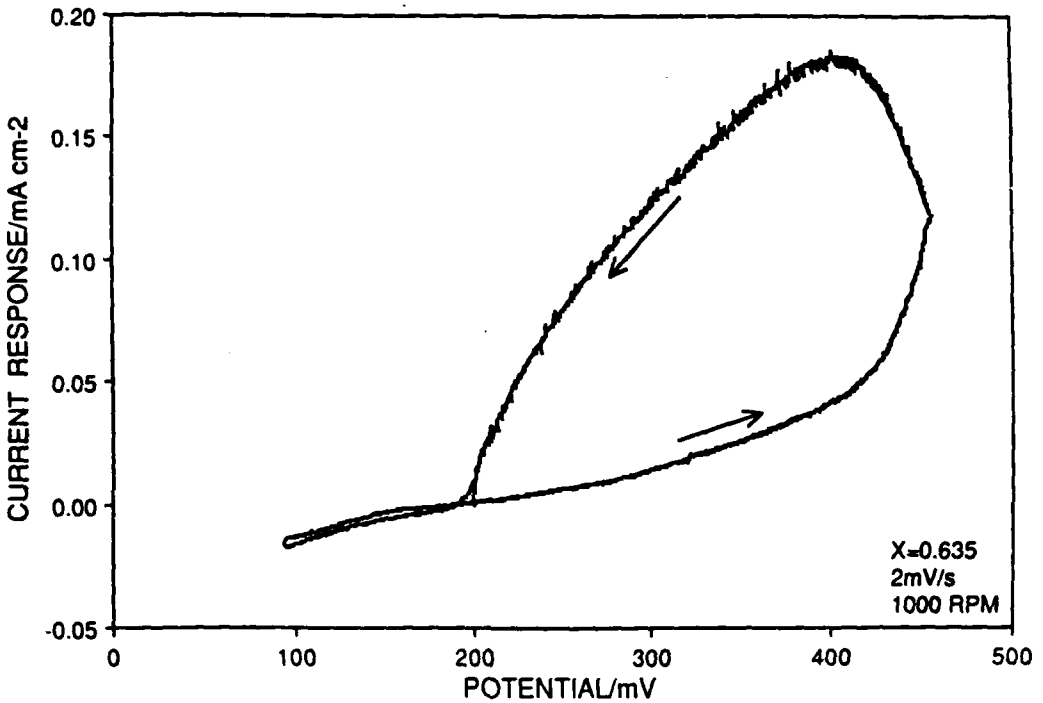

Figure 5. Slow cyclic voltammogram of aluminum rotating cylinder electrode. The anodic switching potential was selected to be less anodic than the current peak in Figure 1.

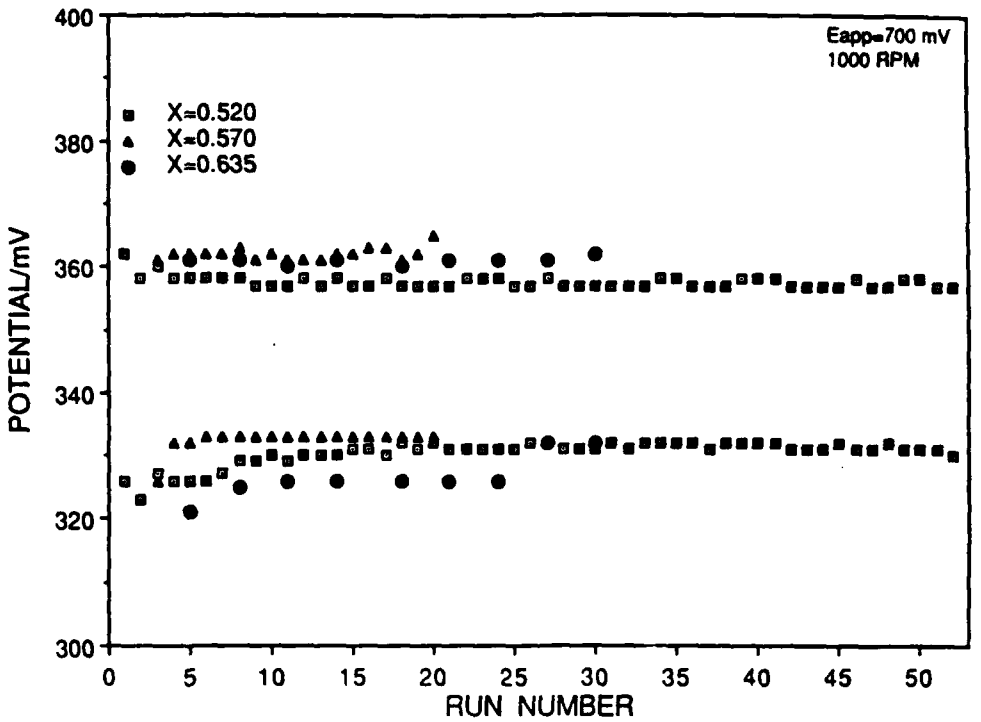

Figure 6. Open circuit potential arrests after a 700 mV potentiostatic step was applied to the working electrode for 100 seconds.

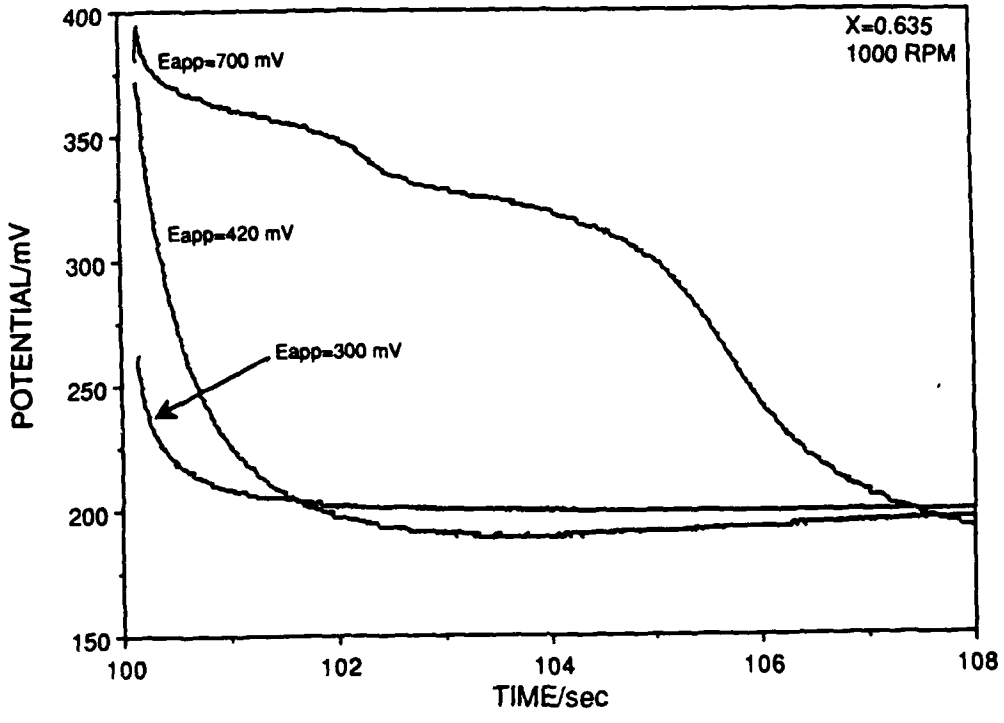

Figure 7. Open circuit potential relaxation of aluminum rotating cylinder electrode after 100 second potentiostatic steps.

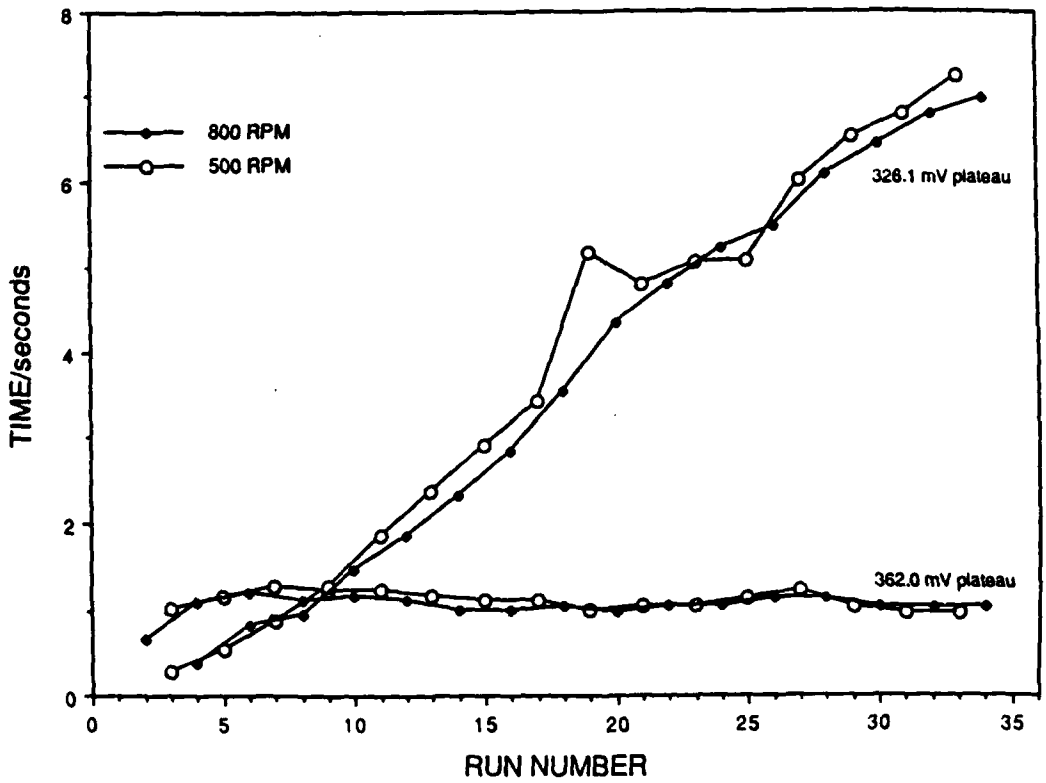

Figure 8. Duration of potential arrests for a passivated aluminum rotating cylinder electrode.

Section 3. Chemistry and Electrochemistry of Aluminum and Its Ions in a Low Temperature Molten Salt With Reactive Solvents

Low temperature molten salts based on mixtures of aluminum chloride and butylpyridinium chloride (BPC) or 1-methyl-3-ethylimidazolium chloride (MEIC) have been suggested as electrolytes for batteries and electrodeposition (1-11). The cationic species for these low temperature molten salts is the organic cation, i.e., butylpyridinium or 1-methyl-3-ethylimidazolium, while the anionic species are Cl^- and $AlCl_4^-$ in basic melts (where the mol fraction of $AlCl_3$, N, is less than 0.50) and $AlCl_4^-$ and $Al_2Cl_7^-$ in acidic melts (where $N > 0.50$) (e. g., see Ref. 12). Addition of organic solvents (e.g., benzene, nitriles) has been shown to improve some transport properties for these melts (1, 13).

The electrochemistry of aluminum has been studied extensively in acidic compositions of these molten salts. Aluminum electrodes have been shown to be reversible at ambient temperature with butylpyridinium cations (1, 5, 9, 10) and 1-methyl-3-ethylimidazolium cations (6, 8). Electrorefining of aluminum has been studied at above-ambient temperatures in $AlCl_3$-MEIC binaries (14). Electrodeposition from basic melts has not been reported. Recent studies have shown that aluminum electrodes undergo passivation in acidic melts when polarized a few hundred millivolts anodic of the equilibrium potential (15).

Aluminum chloride has been found to react with acetonitrile (16-18) and benzonitrile (16) to form cationic and neutral aluminum-containing species as well as $AlCl_4^-$. Identification of the various species were obtained from ^{27}Al nuclear magnetic resonance (nmr) (16-18), and FT-IR and Raman spectra (17, 18). Four cationic aluminum-containing species were identified in 'acidic' ternaries of $N(CH_3)_4Cl$-CH_3CN-$AlCl_3$ (18). The ^{27}Al assignments for the various species are given in Table 1. ^{27}Al nmr spectra have been performed on BPC- (19) and MEIC- (20) $AlCl_3$ binary melts where it was found that the ^{27}Al line width increased with increasing mol fraction of $AlCl_3$ in the acidic region (19, 20).

This paper will present work which examines the formation of aluminum-containing neutral and cationic species as a result of reactions of organic bases with components of aluminum chloride - MEIC low temperature molten salt electrolytes and the influence of these species on the electrochemical characteristics of aluminum electrodes in the resulting ternary solutions.

Experimental

The organic salt was synthesized and purified similarly to the method of Wilkes and coworkers (21). The aluminum chloride (Fluka puriss.) was sublimed from a mixture of NaCl and aluminum wire in an evacuated vessel at 170°C onto a 'cold finger' cooled by an external flow of air. The acetonitrile and butyronitrile were distilled over P_2O_5. The benzonitrile, diethylamine, and triethylamine were dried by storage over molecular sieve (Type 4A). All of the organic solvents were stored in a dry box (separate from the one used for electrochemical measurements) under an atmosphere which was a mixture of nitrogen and helium.

The nmr spectra were obtained on an IBM Model NR/200 FTNMR with a broad-band probe and variable temperature accessory. Each sample was prepared in the aforementioned dry box and placed in a 5 mm tube, covered with a cap, removed from the dry box, and inserted into a 10 mm tube (containing the D_2O used as a lock signal). The spectrometer reference was the frequency of the $Al(D_2O)_6^{3+}$ reference species (22).

The electrochemical measurements were carried out in specially designed cells which provided separate compartments for test, counter, and reference electrolytes. The reference electrode was an aluminum-plated platinum wire immersed in a reference electrolyte which had an $AlCl_3$ mol fraction of 0.505. The aluminum samples used were cylinders (Johnson Matthey m5N, 6.25 mm diameter X 5 mm) which were mounted in specially designed PTFE rotating electrode holders. The top and bottom of the cylinders were not in contact with the electrolyte. When deposition-stripping experiments were carried out, the electrode was a glassy carbon rotating disk (Pine, 5mm diameter). Rotation for both types of electrodes was provided by a Pine Rotator (Model MSR). Potentiostatic control was achieved with a PARC Model 273 Potentiostat-Galvanostat. Potential measurements were made with a Keithley Model 197 Digital Multimeter.

Results

Ternary solutions of MEIC-$AlCl_3$ with acetonitrile were homogeneous at ambient temperatures at low (≤ 0.1) and intermediate (≥ 0.4) mol fractions of CH_3CN. In the region between these low and intermediate CH_3CN mol fractions, two phases (one solid and one liquid) were found. ^{27}Al nmr spectra were obtained on single, liquid phase samples. Ternaries composed of the low temperature molten salt and butyro- and benzo-nitrile were prepared with nitrile compositions similar to those which yielded single phase samples with acetonitrile. Figure 1 shows samples of the ^{27}Al nmr spectra for these nitrile-rich ternaries. The peaks observed for the three nitriles are summarized in Table 2. In all cases, a single, sharp peak was obtained at +102 ppm while a sharp, but

small (the "inserted" spectra are 64X or 128X the "main" spectra), peak was observed in the vicinity of -32 ppm. In the cases of the aliphatic nitriles, a broad (but small) peak was observed at about -22 ppm.

The secondary and tertiary amines were liquid at room temperature, but did not form single phase solutions when mixed with the binary molten salts (at compositions comparable to the nitriles). Instead, two liquid phases were formed; the amines, being less dense than the molten salts, formed the upper phase. Samples were carefully obtained from each of the phases and placed in nmr tubes. The resulting ^{27}Al nmr spectra are shown in Fig. 2 and summarized in Table 3. All of the aluminum species were associated with tetrahedral complexes.

Anodic polarization of aluminum electrodes in acetonitrile-containing ternaries revealed the absence of passivation and an increase in dissolution rate (relative to the binary molten salt) in the potential region above +275 mV. Fig. 3 shows the effect of varying amounts of acetonitrile on the dissolution behavior of aluminum electrodes for ternaries derived from N = 0.58 binary molten salt. Fig. 4 shows the effect of rotation rate (of the aluminum cylinder) on anodic polarization and the 'limiting' current density in the region around +400 mV. Benzonitrile-containing ternaries (mixtures derived from N = 0.58 binary molten salt) yielded curves similar to those shown in Fig. 3, but the increase in current density was not observed until electrode potentials in excess of +400 mV were achieved.

Deposition-stripping experiments were carried out on glassy carbon rotating disk electrodes in contact with acidic binary molten salts and ternaries (mixtures with acidic binary melts) containing acetonitrile and benzonitrile . While aluminum deposition and subsequent dissolution were observed in the cases of the binaries, deposition of aluminum was not observed from ternaries containing the nitriles.

Discussion

The ^{27}Al nmr data shown in Fig. 1 are the first identifications of aluminum-containing, octahedral cationic species in these low temperature molten salts. All of the peaks found in this study have already been identified for CH_3CN or C_6H_5CN - $AlCl_3$ binaries (compare Tables 1 and 2), and those found for the butyronitrile-containing ternaries were close to their CH_3CN or C_6H_5CN analogs. The appearance of a single, sharp line at 102 ppm for all of these spectra was indicative of the absence of $Al_2Cl_7^-$ in the melts. This observation is based on previously reported binary data for ^{27}Al nmr (19, 20) and a correlation obtained in this work (at 24°C) for the variation of line width, λ/ppm, at 102 ppm with $AlCl_3$ mol fraction, N, in the acidic region, i.e..

$$\lambda = -1.75X10^4 + 5.06X10^4\,N - 3.14X10^4\,N^2 \qquad [1].$$

Thus, the nitriles, at these mol fraction levels, must have reacted quantitatively with $Al_2Cl_7^-$ to form the cationic species. The following reactions are consistent with these observations

$$4\,Al_2Cl_7^- + 6\,B = 7\,AlCl_4^- + AlB_6^{3+} \qquad [2]$$

and

$$3\,Al_2Cl_7^- + 5\,B = 5\,AlCl_4^- + AlClB_5^{2+} \qquad [3]$$

where B represents the solvent (base) species. In the cases of the alkanenitriles, the cationic species associated with both reactions were obtained. In the case of benzonitrile, only the chloride-free, aluminum-benzonitrile complex was observed.

^{27}Al nmr data for the interaction of the secondary and tertiary amines in molten salts (Figs. 2b and 2d and Table 3) indicated the absence of octahedral complexes. Further, the movement of the "$AlCl_4^-$" peak upfield for $(C_2H_5)_2NH$ and the sharpening of the "$AlCl_4^-$" peak (along with the appearance of a broad peak downfield) for triethylamine suggest the formation of a neutral adduct, i.e.,

$$Al_2Cl_7^- + B = AlCl_4^- + BAlCl_3 \qquad [4].$$

The peaks found at 108 ppm in the amine-rich and salt-rich phases for $(C_2H_5)_3N$ indicate a non-ionic species while the shift of approximately 6 ppm (with the retention of the relatively broad peak) for "$AlCl_4^-$" in the salt-rich phase (with $(C_2H_5)_2NH$) suggests the same, but with substantial exchange among the species. These peaks are consistent with neutral adducts proposed for benzonitrile (16) and acetonitrile (16-18) reacting with $AlCl_3$. The relatively sharp peak (64 ppm) and the very broad 'peak' (68 ppm) in the amine-rich phase for the secondary and tertiary amines, respectively, suggest an additional neutral species whose identity is unknown.

The aluminum electrode is reversible in binary acidic melts of low temperature molten salts according to

$$Al + 7\,AlCl_4^- = 4\,Al_2Cl_7^- + 3\,e^- \qquad [5].$$

A mechanism for anodic dissolution consistent with this overall reaction would involve a

multiple step process with chloride-containing adsorbed intermediate species. It has been proposed that the adsorbed intermediates (especially those with relatively large surface coverages at high anodic overpotentials, i.e., those species chemically-close to "$AlCl_3$") are the cause of passivation of the aluminum surface during anodic polarization (15). Inspection of Eqs. [2] and [3] shows that the product of the reaction given by Eq. [5] is spontaneously consumed to form aluminum-containing cationic species (in addition to $AlCl_4^-$). Thus, it is feasible that the passivating film could be thermodynamically unstable in the presence of reactive organic bases and dissolve on formation. Alternatively, one could envision direct intervention of the base in the electrochemical dissolution process, e.g.,

$$Al + 6\ B = AlB_6^{3+} + 3\ e^- \qquad [6]$$

and

$$Al + 1/3\ AlCl_4^- + 20/3\ B = 4/3\ AlClB_5^{2+} + 3\ e^- \qquad [7],$$

essentially eliminating the chloride-containing adsorbed intermediate species. It is evident from Figs. 3 and 4 that the presence of acetonitrile substantially increases the aluminum dissolution rate.

Examination of the data contained in Figs. 3 and 4 reveals that the electrode potential where the dissolution rate increased was more-or-less independent of the original (binary) composition of the molten salt. Further, the magnitude of the anodic current density (at a fixed potential) was dependent upon the amount of acetonitrile present. Both observations tend to support the premise that acetonitrile was involved directly in the dissolution process (e.g., see Eq [6]).

At about +400 mV the dissolution rate became potential-independent, i.e., there was an apparent limiting current density. The more-than threefold increase in limiting current density with slight increase of the concentration of acetonitrile for ternaries derived from N = 0.58 binaries (Fig. 3) indicated that mass transport of CH_3CN was an unlikely cause of the limiting rate. Similarly, doubling the rotation rate for the ternary derived from N = 0.51 resulted in a nearly-threefold increase in rate (Fig. 4) which was significantly larger than would be expected for mass transport control. The strong influence of CH_3CN concentration on the rate (Fig. 3) supports the contention of direct involvement in the dissolution process. Full understanding of the enhanced dissolution rate and limiting current density is not available at this time.

As noted above, similar electrochemical behavior was observed for benzonitrile-containing ternaries. However, the effect was observed only at (and above) potentials where the apparent limiting current density was observed in CH_3CN ternaries.

On the basis of the ^{27}Al nmr spectra of the ternaries containing nitriles (Fig. 1), the only aluminum-containing species present in those solutions was $AlCl_4^-$ and the complexed cations. Therefore, electrodeposition of aluminum can not occur by the reverse of Eq. [5]. Deposition of aluminum has only been observed in low temperature molten salts where $Al_2Cl_7^-$ is present, i.e., deposition does not take place when the source of aluminum is $AlCl_4^-$. Therefore, a necessary condition for deposition from these ternaries is the reverse of reactions like those given by Eqs. [6] and [7]. Since electrodeposition of aluminum was not observed with ternaries containing either CH_3CN or C_6H_5CN, one must conclude that deposition from the cationic complexes does not occur.

In order to determine the relative stabilities of the aluminum-containing ionic species in the presence of acetonitrile, MEIC was added to a ternary solution (Fig. 1a) in sufficient amount to yield an equivalent "binary" of N = 0.45. The resulting ^{27}Al nmr spectrum revealed only the presence of $AlCl_4^-$, i.e., the chloride ions reacted with the cationic species to form $AlCl_4^-$ and free CH_3CN. One concludes that the relative stabilities of the aluminum-containing species are $Al_2Cl_7^- < Al(CH_3CN)_6^{3+} \approx AlCl(CH_3CN)_5^{2+} < AlCl_4^-$.

Conclusions

Excess amounts (i.e., above stochiometric requirements) of organic bases (alkanenitriles, benzonitrile, and di- and tri-ethylamine) have been shown to react quantitatively with $Al_2Cl_7^-$ in acidic mixtures of low temperature molten salts. The reactions led to the formation of octahedral aluminum-containing cationic species in the cases of nitriles and in tetrahedral aluminum-containing neutral species in the cases of the amines. The observed relative stabilities of aluminum-containing species in ternaries with acetonitrile were $Al_2Cl_7^- < Al(CH_3CN)_6^{3+} \approx AlCl(CH_3CN)_5^{2+} < AlCl_4^-$.

Electrodissolution of aluminum was found to be facilitated at high electrode potentials in nitrile-containing ternaries and passivation of the metal surface was not observed. Electrodeposition of aluminum from the nitrilo-containing cationic complexes was not observed.

Table 1. Literature Assignments of ^{27}Al NMR Chemical Shifts of Aluminum-Containing Species.

Species	Chemical Shift (ppm)	Reference(s)
$AlCl_4^-$	+102	16, 17
$Al_2Cl_7^-$	+102	--
$AlCl_3C_6H_5CN$	+98	16
$AlCl_3CH_3CN$	+87/+96	16/17
$Al(D_2O)_6^{3+}$	0	--
$Al(CH_3CN)_5^{3+}$	-12	16, 17
$AlCl_2(CH_3CN)_4^+$	-14	16, 17
$AlCl_n(C_6H_5CN)_{6-n}^{+3-n}$	-18	16
$AlCl(CH_3CN)_5^{2+}$	-24	16, 17
$Al(C_6H_5CN)_6^{3+}$	-29	16
$Al(CH_3CN)_6^{3+}$	-34	16, 17

Table 2. Observed ^{27}Al NMR Chemical Shifts in $AlCl_3$-MEIC-Nitrile Ternaries.

Nitrile	Peaks Observed (ppm)
Aceto-	+102
	-23
	-34
Butyro-	+103
	-21
	-34
Benzo-	+102
	-31

Table 3. Observed ^{27}Al NMR Chemical Shifts in $AlCl_3$ (N = 0.58)-MEIC Binaries in Contact with Amines.

Amine	Amine Phase	Salt Phase
Diethyl	+64	+96
Triethyl	+109	+107
	+68	+102

References

1. J. Robinson and R. A. Osteryoung. **This Journal, 127**, 122 (1980)

2. R. A. Carpio, L. A. King, R. E. Lindstrom, J. C. Nardi, and C. L. Hussey. **ibid., 126**, 1644 (1979).

3. A. A. Fannin, L. A. King, J. A. Leviskey, and J. S. Wilkes. **ibid., 88**, 2614 (1984).

4. A. A. Fannin, D. A. Floreani, L. A. King, J. S. Landers, B. J. Piersma, D. J. Stech, R. L. Vaughn, J. S. Wilkes, and J. L. Williams. **J. Phys. Chem., 88**, 2614 (1984).

5. Q-X. Qin and M. Skyllas-Kazacos. **J. Electroanal. Chem., 168**, 193 (1984).

6. J. J. Auborn and Y. L. Barberio. **This Journal, 132**, 598 (1985).

7. P. G. Pickup and R. A. Osteryoung. **J. Electroanal. Chem., 195**, 271 (1985).

8. G. F. Reynolds and C. J. Dymek. **J. Power Sources, 15**, 109 (1985).

9. P. K. Lai and M. Skyllas-Kazacos. **Electrochim. Acta, 32**, 1443 (1987).

10. Y. Chryssoulakis, J-C. Poignet, and G. Manoli. **J. Appl. Electrochem., 17**, 857 (1987).

11. C. J. Dymek, G. F. Reynolds, and J. S. Wilkes. **This Journal, 134**, 1658 (1987).

12. R. J. Gale and R. A. Osteryoung. **Inorg. Chem., 18**, 1603 (1979).

13. A. A. Fannin, D. A. Floreani, L. A. King, J. S. Landers, B. J. Piersma, D. J. Stech, R. L. Vaughn, J. S. Wilkes, and J. L. Williams. **Technical Report. FJSRL-TR-82-0006.** F. J. Seiler Research Laboratory. USAF Academy (CO), 1982.

14. F. M. Donahue. **Electrochem. Soc. Extended Abstracts. Vol. 86-2.** San Diego (CA), Oct. 19-24, 1986. p. 990.

15. R. Moy, L. R. Simonsen, and F. M. Donahue. **Electrochem. Soc. Extended Abstracts. Vol. 86-2.** San Diego (CA), Oct. 19-24, 1986. pp. 138-9.

16. F. W. Wehrli and R. Hoerdt. **J. Magn. Reson., 42**, 334 (1981).

17. M. Dalibart, J. Derouault, P. Granger, and S. Chapelle. **Inorg. Chem., 21**, 1040 (1982).

18. M. Dalibart, J. Derouault, and P. Granger. **ibid., 21**, 2241 (1982).

19. J. L. Gray and G. E. Maciel. **J. Am. Chem. Soc., 103**, 7147 (1981).

20. J. S. Wilkes, J. S. Frye, and G. F. Reynolds. **Inorg. Chem., 22**, 3870 (1983).

21. J. S. Wilkes, J. A. Levisky, R. A. Wilson, and C. L. Hussey. **Inorg. Chem., 21**, 1263 (1982).

22. C. Brevard and P. Granger. **Handbook of High Resolution Multinuclear NMR.** Wiley Interscience, New York, 1981. p. 98.

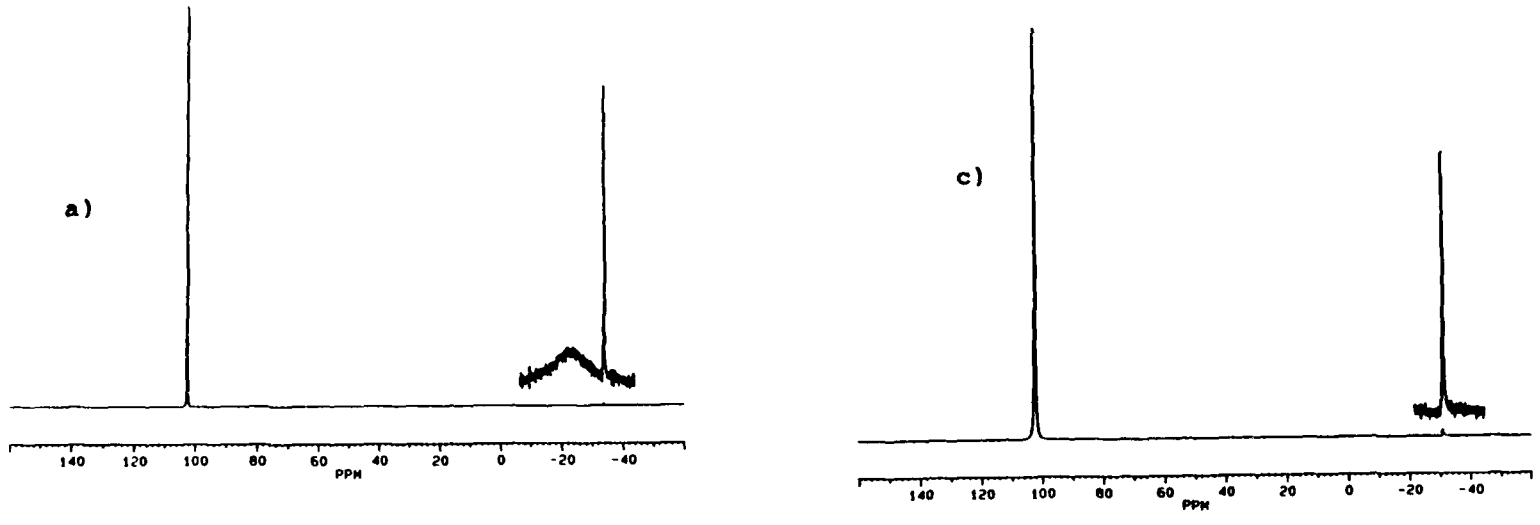

Figure 1. ^{27}Al Nuclear Magnetic Resonance Spectra of Ternaries Made With Nitrile Solvents and $AlCl_3$-MEIC Melts. Temperature = 50°C.
a) N = 0.58 + 36 w/o Acetonitrile;
b) N = 0.58 + 47 w/o Butyronitrile;
c) N = 0.58 + 47 w/o Benzonitrile;
d) N = 0.52 + 27 w/o Acetonitrile.

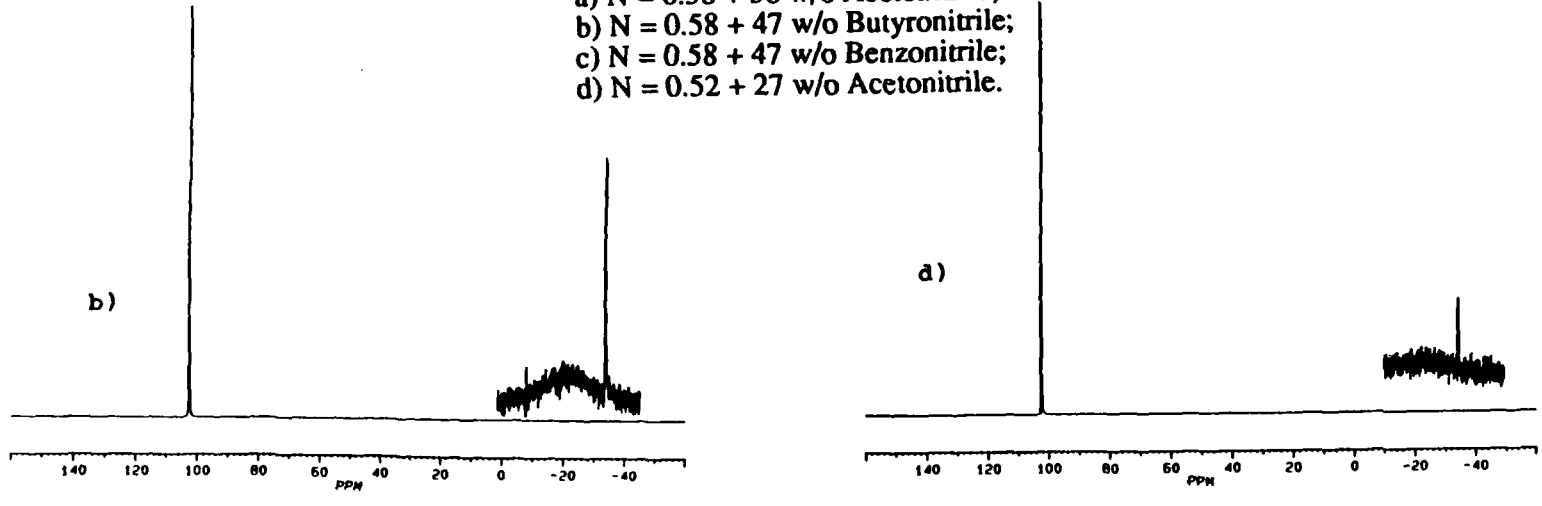

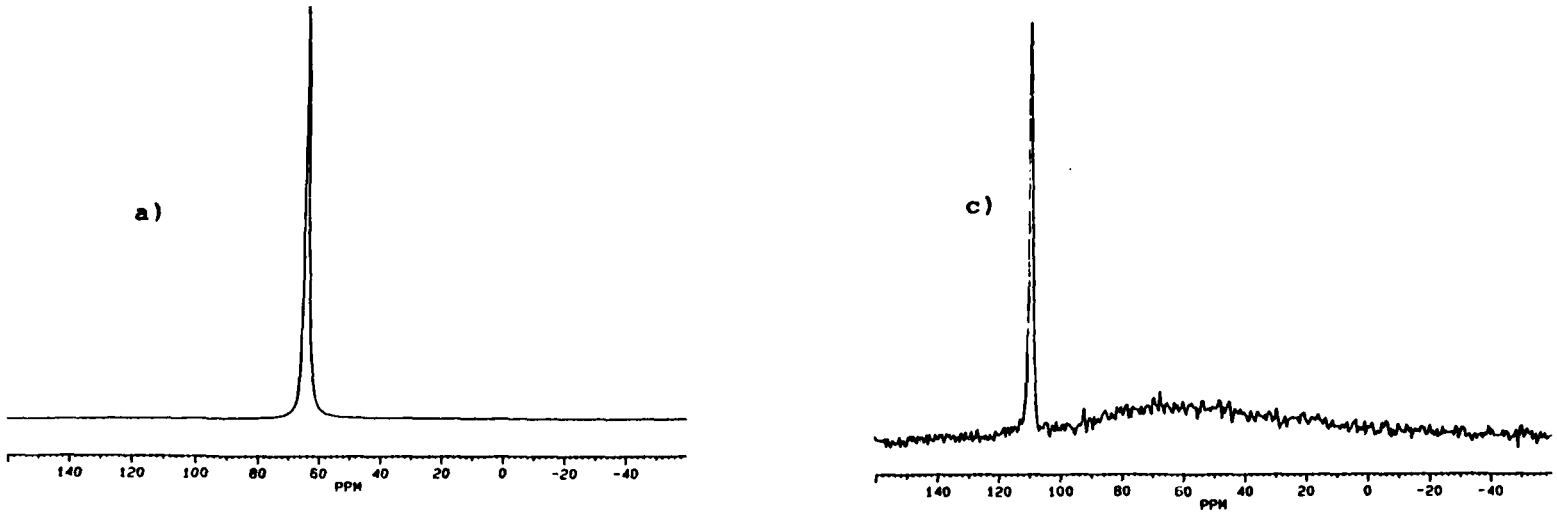

Figure 2. ^{27}Al NMR Spectra of Mixtures of Amines and $AlCl_3$ (N = 0.58) - MEIC Molten Salts. Temperature = 25°C.

a) Diethylamine; amine phase;
b) Diethylamine; salt phase;
c) Triethylamine; amine phase;
d) Triethylamine; salt phase.

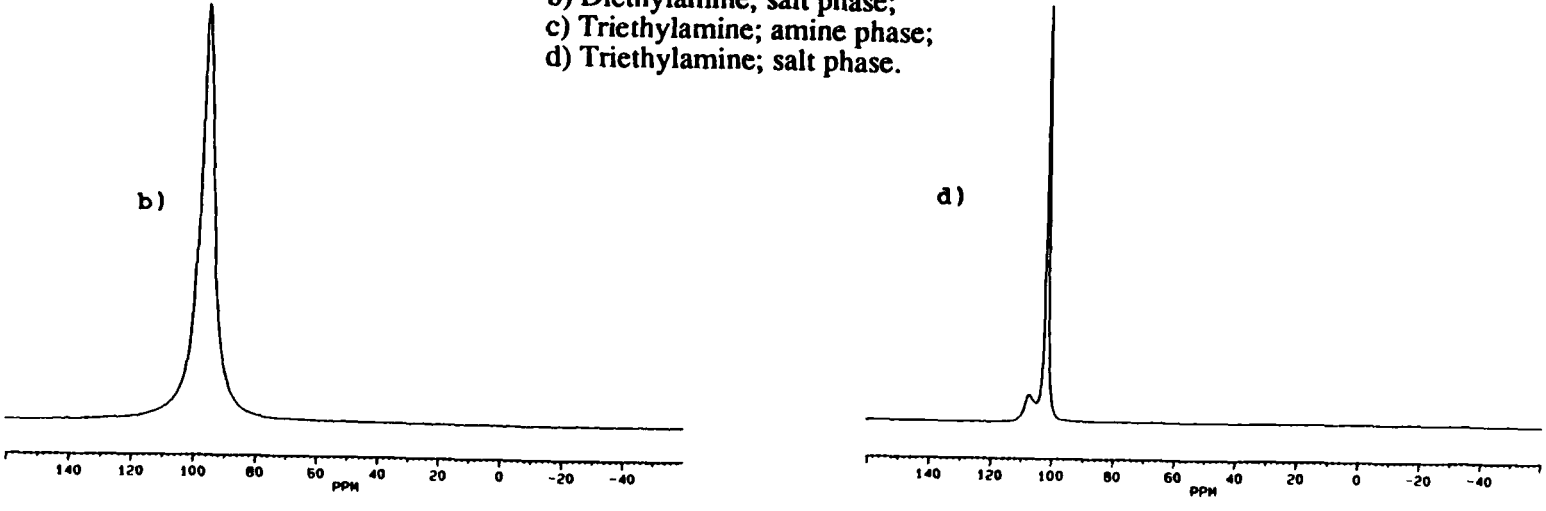

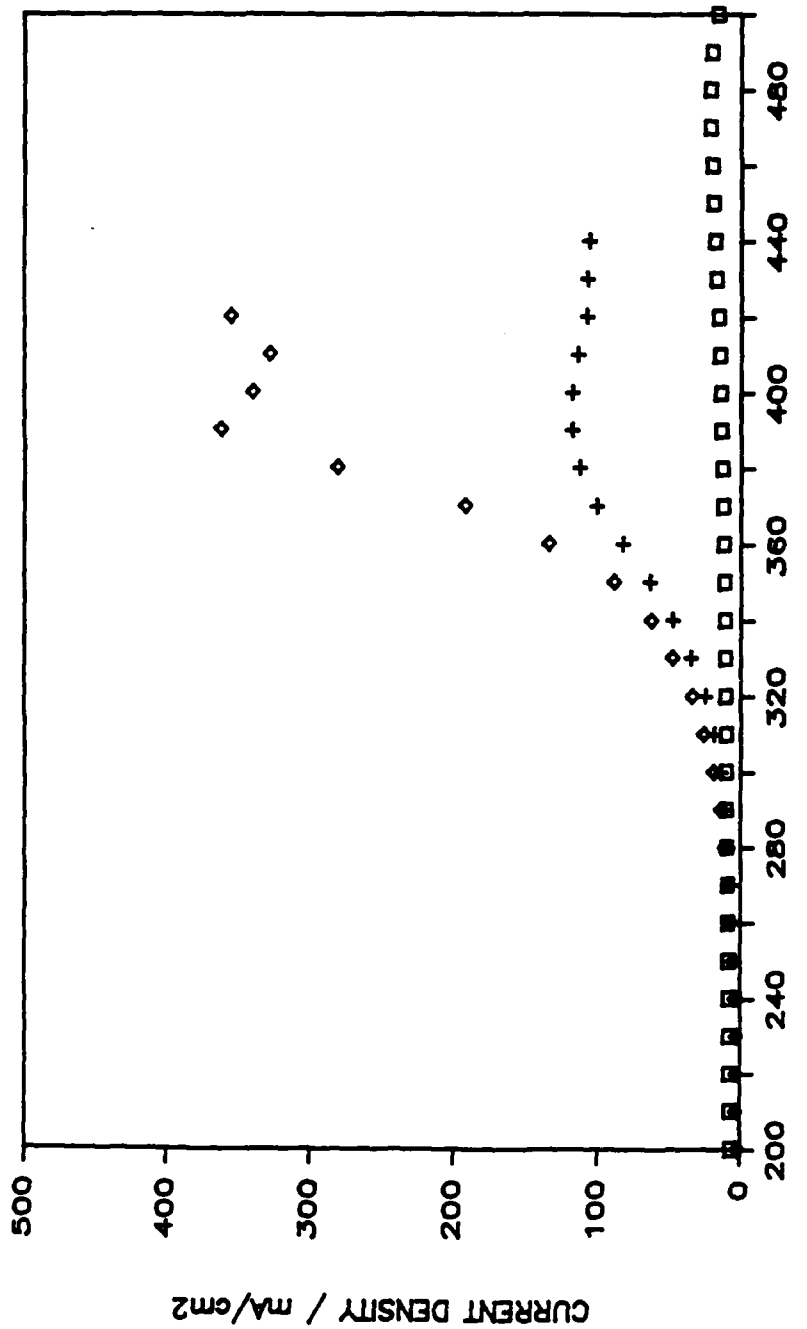

Figure 3. Anodic Polarization of Aluminum in Ternaries Containing Acetonitrile. Sweep Rate = 5 mV/s; Cylinder Rotation Rate = 1000 rpm; Temperature = 30°C.

squares, N = 0.58;
crosses, N = 0.58 + 37 w/o CH_3CN;
diamonds, N = 0.58 + 47.3 w/o CH_3CN.

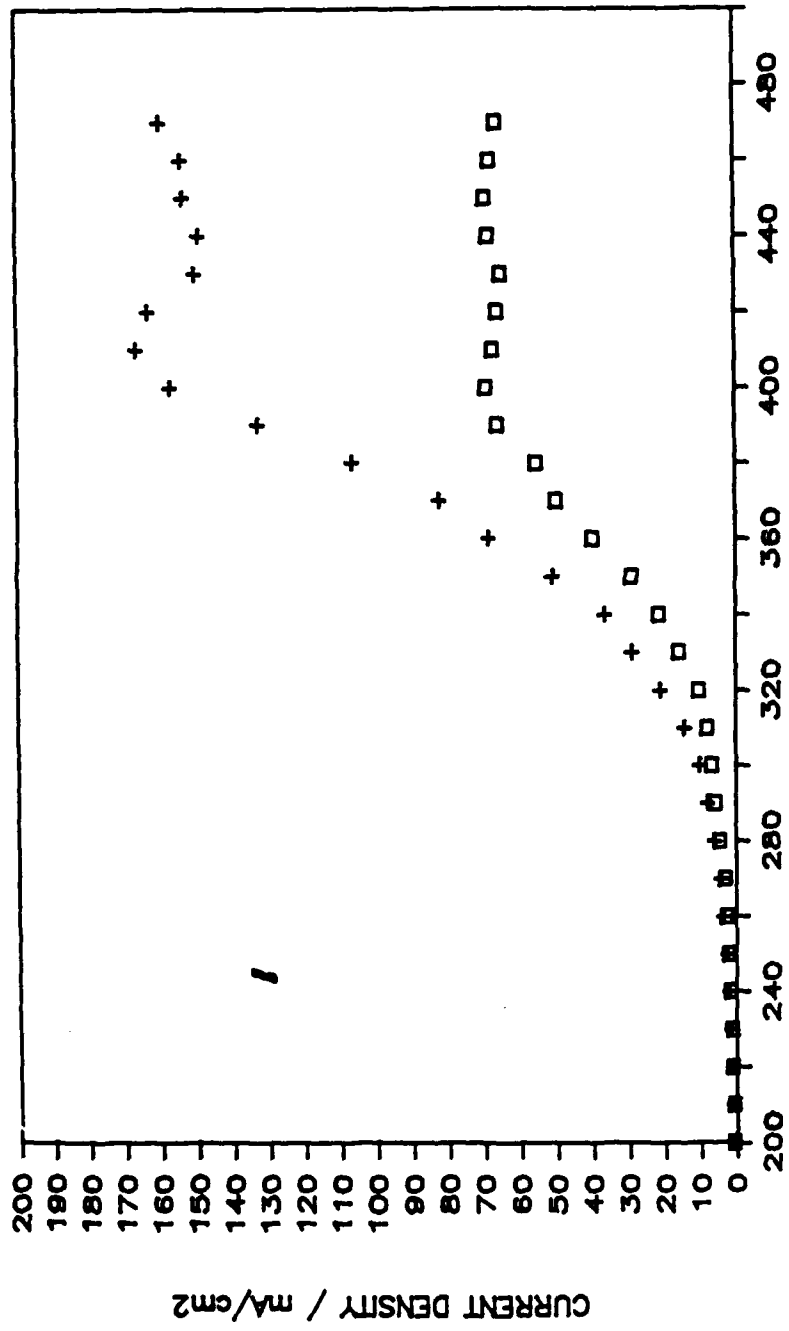

Figure 4. Anodic Polarization of Aluminum in Ternaries Containing Acetonitrile (N = 0.51 + 25 w/o AN). Sweep Rate = 5 mV/s; Temperature = 30°C. squares, Cylinder Rotation Rate = 1000 rpm; crosses, Cylinder Rotation Rate = 2000 rpm.

Section 4. Zinc Dissolution and Transport Processes in Low Temperature Molten Salts

Basic Melts

The dissolution of zinc metal in basic melt compositions is currently under investigation. Preliminary experiments revealed that the zinc dissolution process was irreversible in basic melt compositions, as is the aluminum dissolution process. It was discovered that the dissolution rate of zinc is approximately twenty times greater than that of aluminum in the same melt compositions. Early experiments also revealed the presence of a limiting current region in many of the basic melt compositions which would indicate mass transport control of the dissolution process.

Efforts to produce a reversible zinc dissolution process in basic melt compositions included the addition of $ZnCl_2$, ZnF_2, and $Zn(CN)_2$ to the basic melts. All salts were soluble in the basic compositions. In all cases it was not possible to deposit zinc from basic melts.

Proton NMR spectroscopy was used for verification of melt composition. Correlations were made between the chemical shift of the proton of the number two carbon and both $AlCl_3$ mole fraction (Figure 1) and Cl^- concentration (Figure 2). An attempt to conduct ^{67}Zn NMR experiments in these melts resulted in a very weak signal in only the most concentrated solutions (1 M), with no notable signal being received in the more dilute solutions.

The developed correlation of proton chemical shift and Cl^- concentration was also used as a tool in the determination of zinc coordination numbers in basic melt compositions. Zinc(II) chloride was added to a melt with mole fraction, X, of aluminum chloride of 0.40 and the change in chloride ion concentration was monitored. It was found that at low chloride ion concentrations the coordination number of chloride ion for zinc changed from four to three (Figure 3).

Initial zinc single electrode studies focused on the determination of the diffusivity, D, of the chloride ion, the mass transport limiting specie in the zinc dissolution process. Rotating cylinder electrodes were chosen for these experiments due their relative insensitivity to changes in the electrode surface morphology (e.g. surface roughening) during the dissolution process, and the existence of mass transport correlations.

Experiments were conducted that measured limiting currents as a function of rotation rates in melts with compositions of X=0.485, 0.490, and 0.495 (Figure 4). Measurements were also made in ternary solutions which contained both 5 and 13 weight percent acetonitrile. The existence of two limiting current regions was revealed in the binary melts (Figure 5). It is proposed that the lower limiting current region corresponds to the following reaction:

$$Zn + 4Cl^- \rightarrow ZnCl_4^{2-} + 2e^- \qquad [1],$$

while the upper limiting current corresponds to:

$$Zn + 3Cl^- \rightarrow ZnCl_3^- + 2e^- \qquad [2].$$

The ratio of these limiting currents was found to be equal to the inverse of the stoichiometric coefficient (4:3). Initial calculations have indicated that the quantity $D\mu/T$ is equal to 3.5×10^{-10} g cm/s^2 K, which corresponds to a chloride ion radius of 2.1×10^{-8} cm and suggests that the chloride ion diffuses as a solitary ion and not as an ion aggregate. Diffusivity measurements in the acetonitrile containing solutions were virtually the same as those of the binary solutions which indicated that in basic compositions acetonitrile acted as a non-reactive cosolvent serving to reduce solution viscosity and improve the transport properties of the solution.

The kinetics of the zinc dissolution process has been examined. Binary melts of compositions X= 0.35, 0.375, 0.40, 0.425, and 0.45 have been studied (Figure 6), as well as melts of composition X= 0.40 and 0.45 containing $ZnCl_2$. Preliminary calculations have found that the anodic Tafel slope, β_a, is 17 mV with an exchange current density of 0.1 mA/cm^2. Both of these values have been shown to be independent of melt composition. A complete analysis of the kinetic data has also not yet been finished.

Acidic Melts

A preliminary study of the dissolution of zinc in acidic melts was undertaken. It was found that the zinc dissolution process underwent a passivation process similar to that of aluminum (Figure 7). Experiments revealed that zinc dissolution occurred at a rate ten times greater than that of aluminum. The deposition of zinc was found to occur with the

co-deposition of aluminum. Solubility studies of $ZnCl_2$ in acidic melts revealed that the salt was soluble in concentrations of 50 to 100 mM.

FIG 1. CHEM. SHIFT VS. MOL FRACT. ALCL3

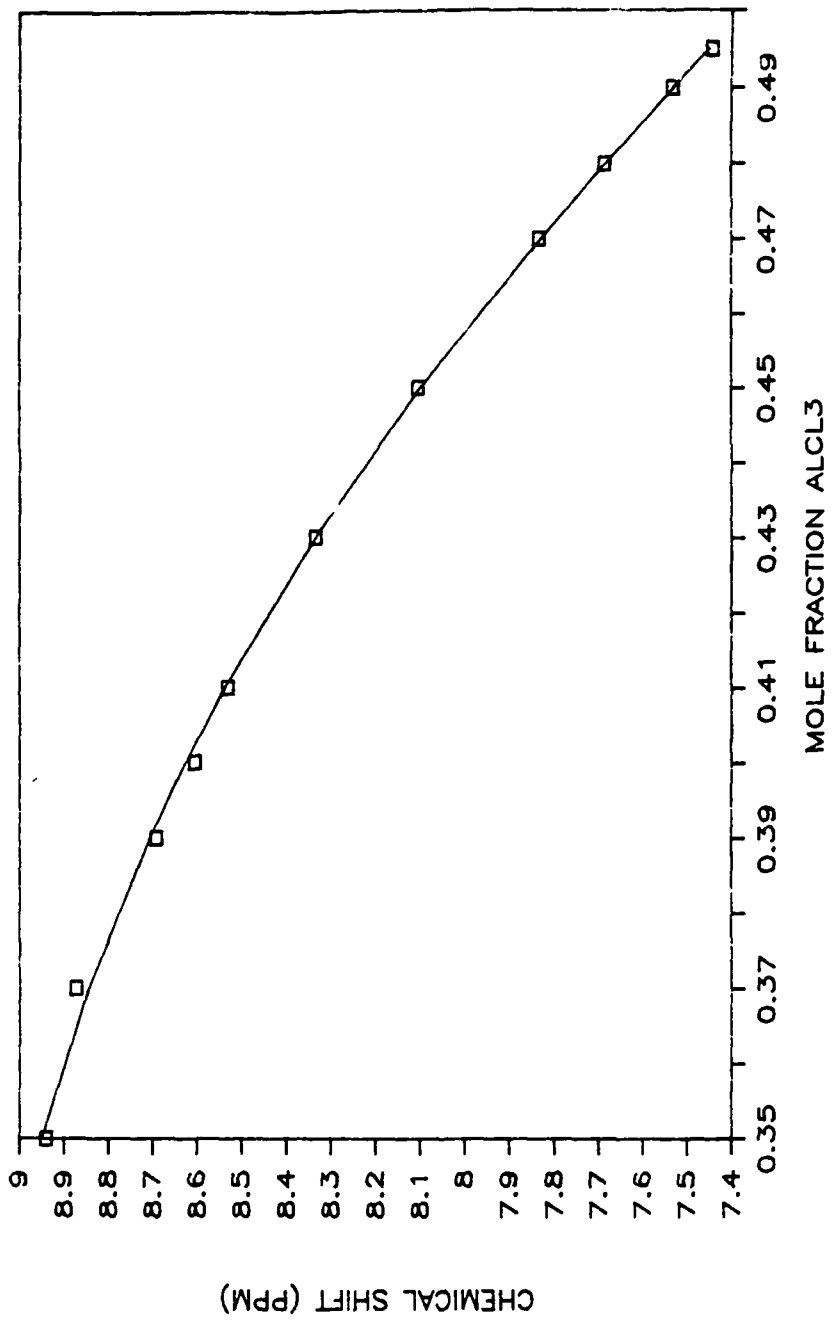

FIG 2. CHEM. SHIFT VS. CL- CONC.

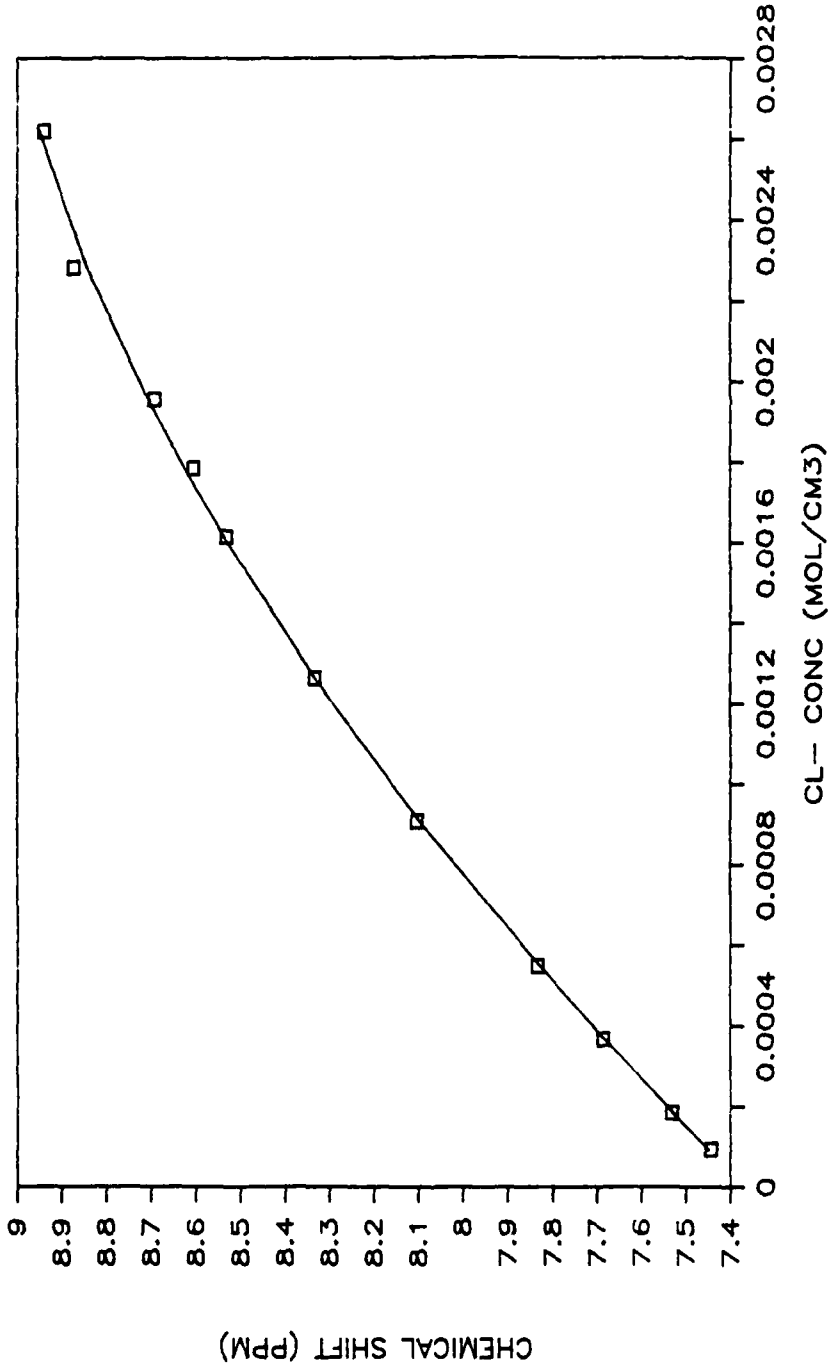

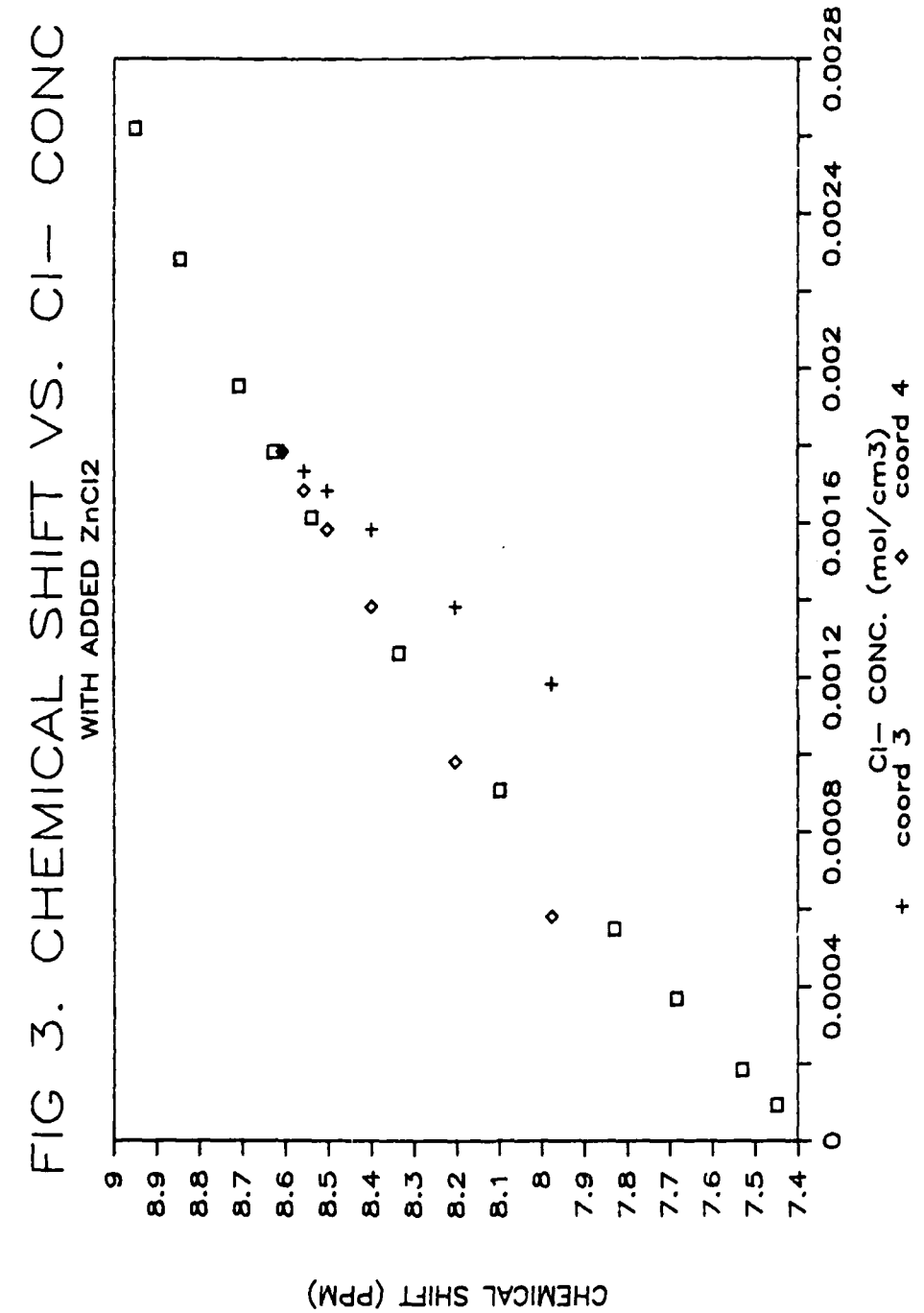
FIG 3. CHEMICAL SHIFT VS. Cl− CONC
WITH ADDED ZnCl2
CHEMICAL SHIFT (PPM)
9
8.9
8.8
8.7
8.6
8.5
8.4
8.3
8.2
8.1
8
7.9
7.8
7.7
7.6
7.5
7.4
0
0.0004
0.0008
0.0012
0.0016
0.002
0.0024
0.0028
Cl− CONC. (mol/cm3)
+ coord 3
◇ coord 4

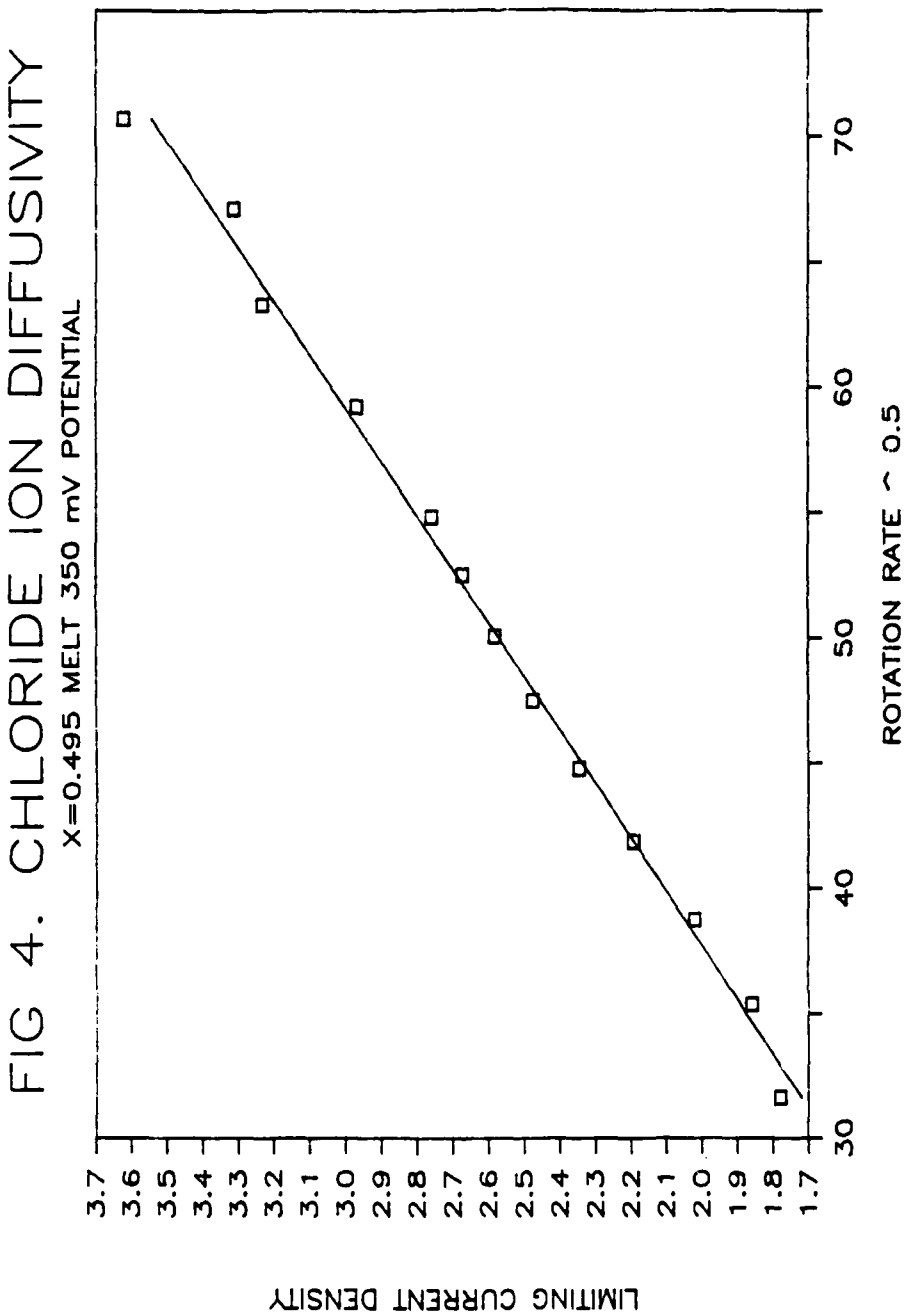
FIG 4. CHLORIDE ION DIFFUSIVITY
X=0.495 MELT 350 mV POTENTIAL
LIMITING CURRENT DENSITY
3.7
3.6
3.5
3.4
3.3
3.2
3.1
3.0
2.9
2.8
2.7
2.6
2.5
2.4
2.3
2.2
2.1
2.0
1.9
1.8
1.7
30
40
50
60
70
ROTATION RATE ~ 0.5

FIG. 5 ZINC DISSOLUTION

1000 RPM X=.485 MELT 25 c

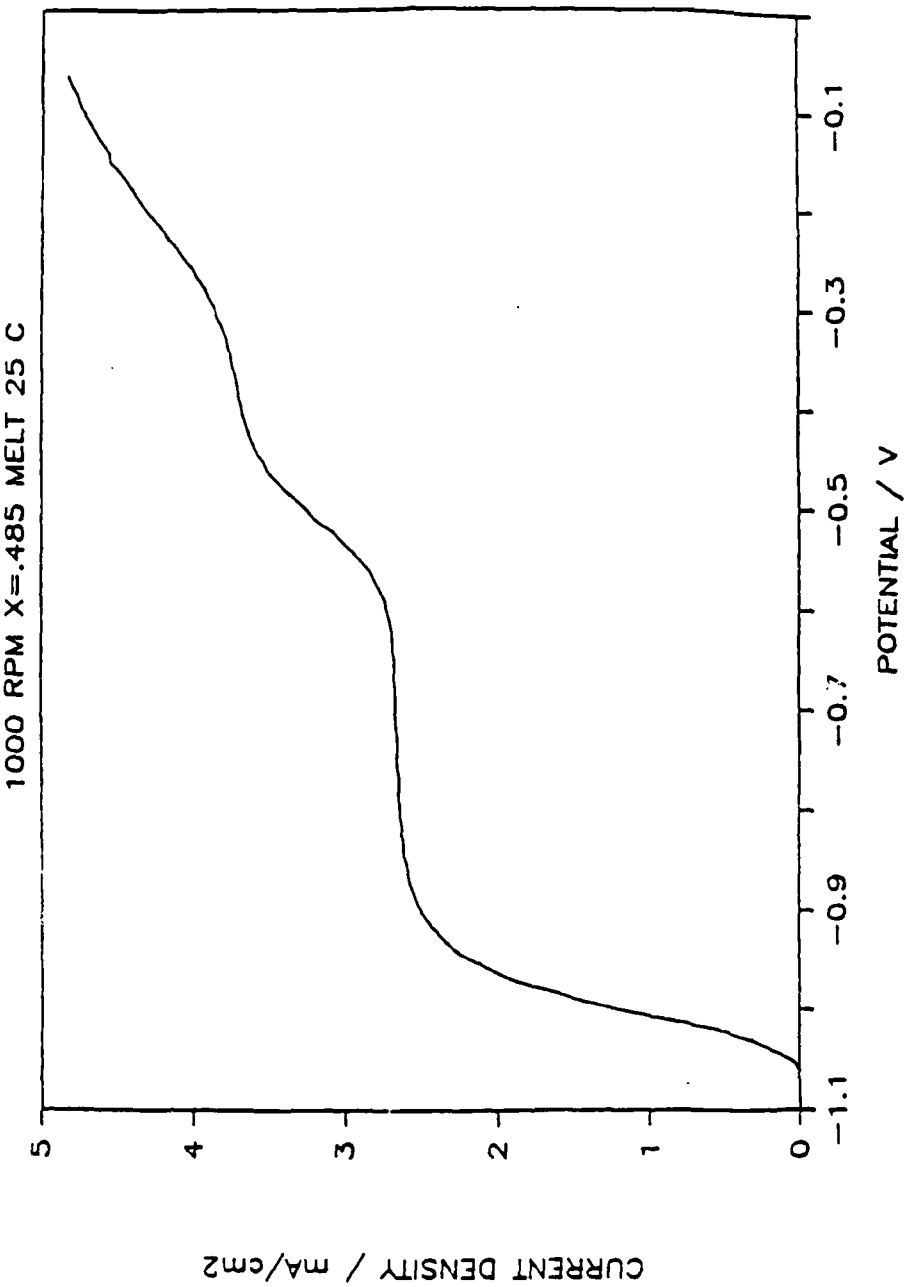

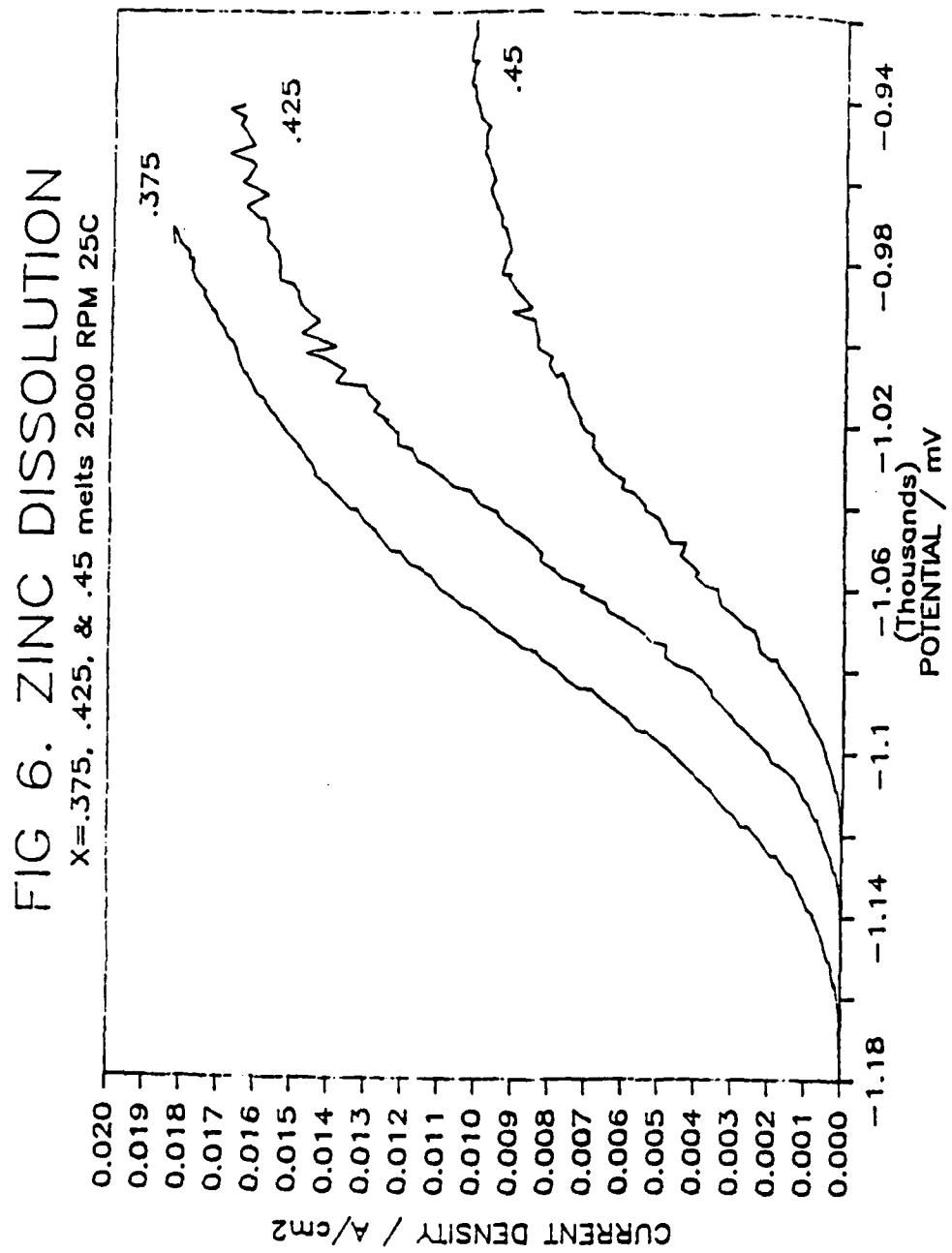
FIG 6. ZINC DISSOLUTION
X=.375, .425, & .45 melts 2000 RPM 25C
.375
.425
.45
CURRENT DENSITY / A/cm2
0.020
0.019
0.018
0.017
0.016
0.015
0.014
0.013
0.012
0.011
0.010
0.009
0.008
0.007
0.006
0.005
0.004
0.003
0.002
0.001
0.000
-1.18
-1.14
-1.1
-1.06
-1.02
-0.98
-0.94
(Thousands)
POTENTIAL / mV

FIG. 7 ZINC DISSOLUTION

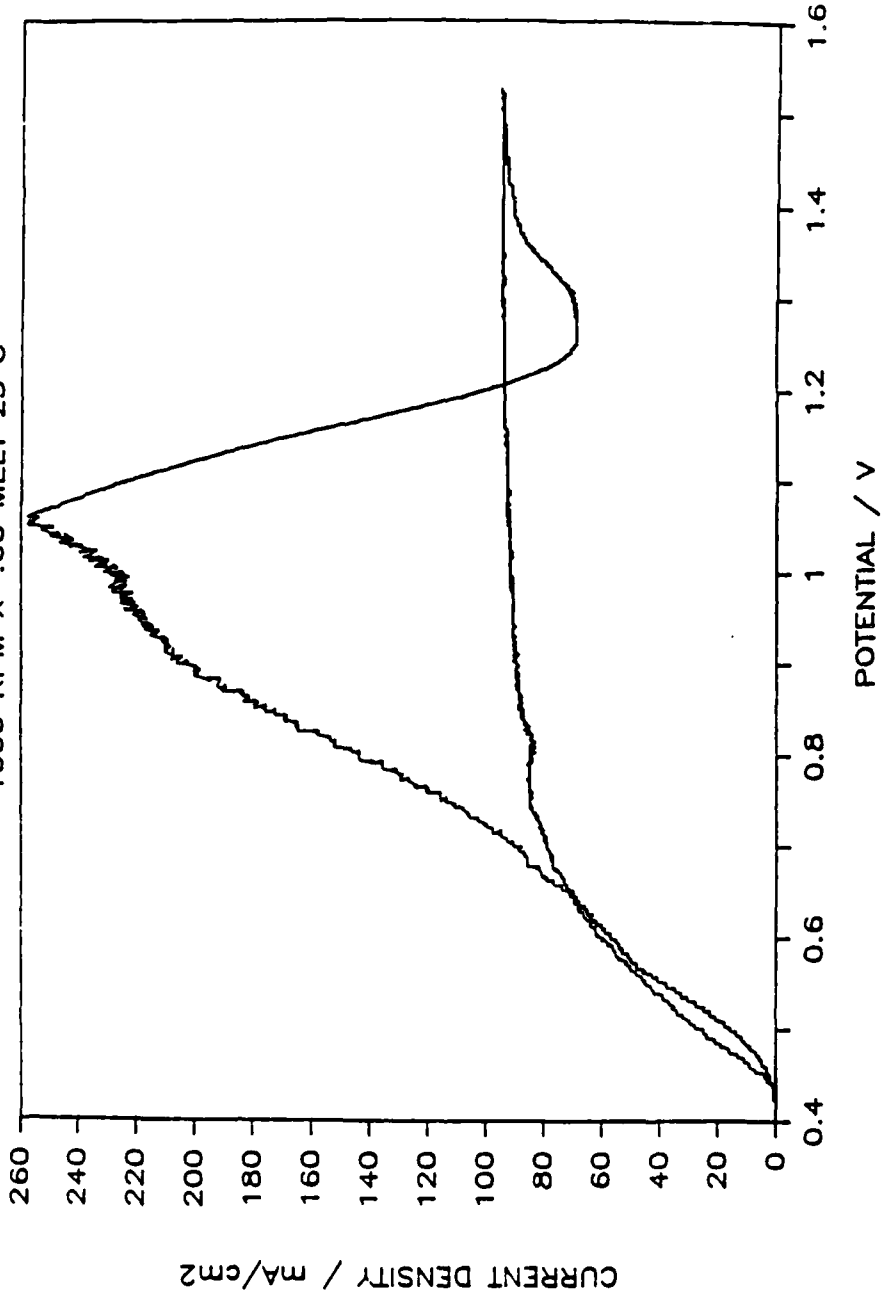

Section 5. Magnesium Dissolution in Binary and Ternary Solutions

The electrodissolution of magnesium in mixtures of aluminum chloride and 1-methyl-3-ethylimidazolium chloride was studied. Both a basic melt, 0.40 mole fraction aluminum chloride, and an acidic melt, 0.58 mole fraction of aluminum chloride, were chosen for analysis. Additionally, the effect of cosolvent, acetonitrile, to both the acidic and basic melts was studied.

The magnesium single electrode studies were carried out at a rotating cylinder electrode at four rotation rates, 1000, 2000, 3000, and 4000 rpm. These rotation rates were high enough to insure establishment of turbulent flow.

In the binary acidic melt, 0.58 mole fraction aluminum chloride, the magnesium electrode reacted spontaneously with the melt (specifically, $Al_2Cl_7^-$) to form metallic aluminum on its surface and exhibited behavior similar to an aluminum electrode in an acidic binary melt. The open circuit potentials of this system were about - 0.1 V, similar to that of an aluminum electrode in the same solution.

This aluminum-like behavior was not observed in the acidic ternary melts. This is believed to be due to the absence of the $Al_2Cl_7^-$ species in the acetonitrile-containing solutions. Acetonitrile added to these melts reacts according to the following :

$$4\ Al_2Cl_7^- + 6\ CH_3CN \rightarrow 7\ AlCl_4^- + Al(CH_3CN)_6^{3+}$$

$$3\ Al_2Cl_7^- + 5\ CH_3CN \rightarrow 5\ AlCl_4^- + AlCl(CH_3CN)_5^{2+}.$$

Thus the source of aluminum for deposition onto the electrode surface is no longer present. Five compositions of the ternary melt were examined, 0.60, 0.65, 0.69, 0.73, and 0.80 mole fraction acetonitrile. The mean open circuit potentials were -1.40 V and showed no systematic dependence on CH_3CN mole fraction. Figure 1 is representative of the current potential behavior of magnesium in the acidic ternary melt. For the lower mole fractions of acetonitrile, the current potential curves exhibited two peak currents while for the larger mole fractions there was only one peak current over a range of 500 mV positive of the open circuit potential. This behavior was the same at each of the four rotation rates but with successively larger peak currents. For the largest mole fraction of acetonitrile the peak current was greatly increased in comparison with the behavior at the other compositions and also occurred at a more positive potential. Observation of the electrode after scanning a particular ternary at each of the rotation rates indicated a very rough surface with a reduced surface area. A new electrode was employed for each series of scans.

In the basic binary melt, 0.40 mole fraction aluminum chloride, the open circuit potential was -1.93 V. The current potential curves exhibited maximum current densities

of 30 mA/cm^2. The ternary melts containing 0.60, 0.65, and 0.75 mole fraction acetonitrile exhibited an average open circuit potential of -1.85 V with a single peak in the current potential curve at -1.5 V. Maximum current densities of 450 mA/cm^2 were measured. Figure 2 is representative of the current potential behavior in both the binary and the ternary basic solutions. Magnesium corroded spontaneously in a 0.40 melt with formation of an orange (cation decomposition) product in the melt.

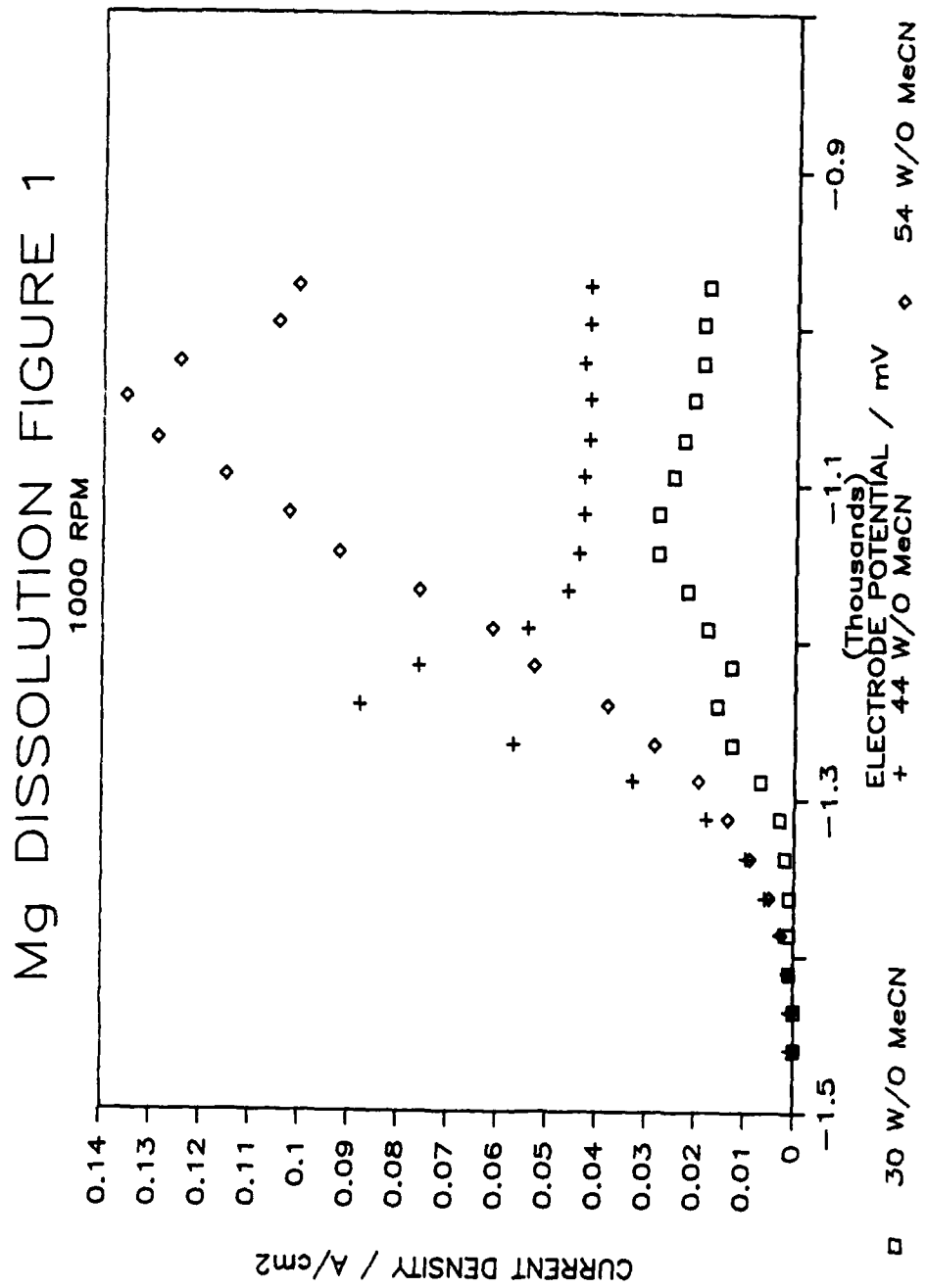
Mg DISSOLUTION FIGURE 1
1000 RPM
CURRENT DENSITY / A/cm2
0.14
0.13
0.12
0.11
0.1
0.09
0.08
0.07
0.06
0.05
0.04
0.03
0.02
0.01
0
−1.5
−1.3
−1.1
−0.9
(Thousands)
ELECTRODE POTENTIAL / mV
30 W/O MeCN
44 W/O MeCN
54 W/O MeCN

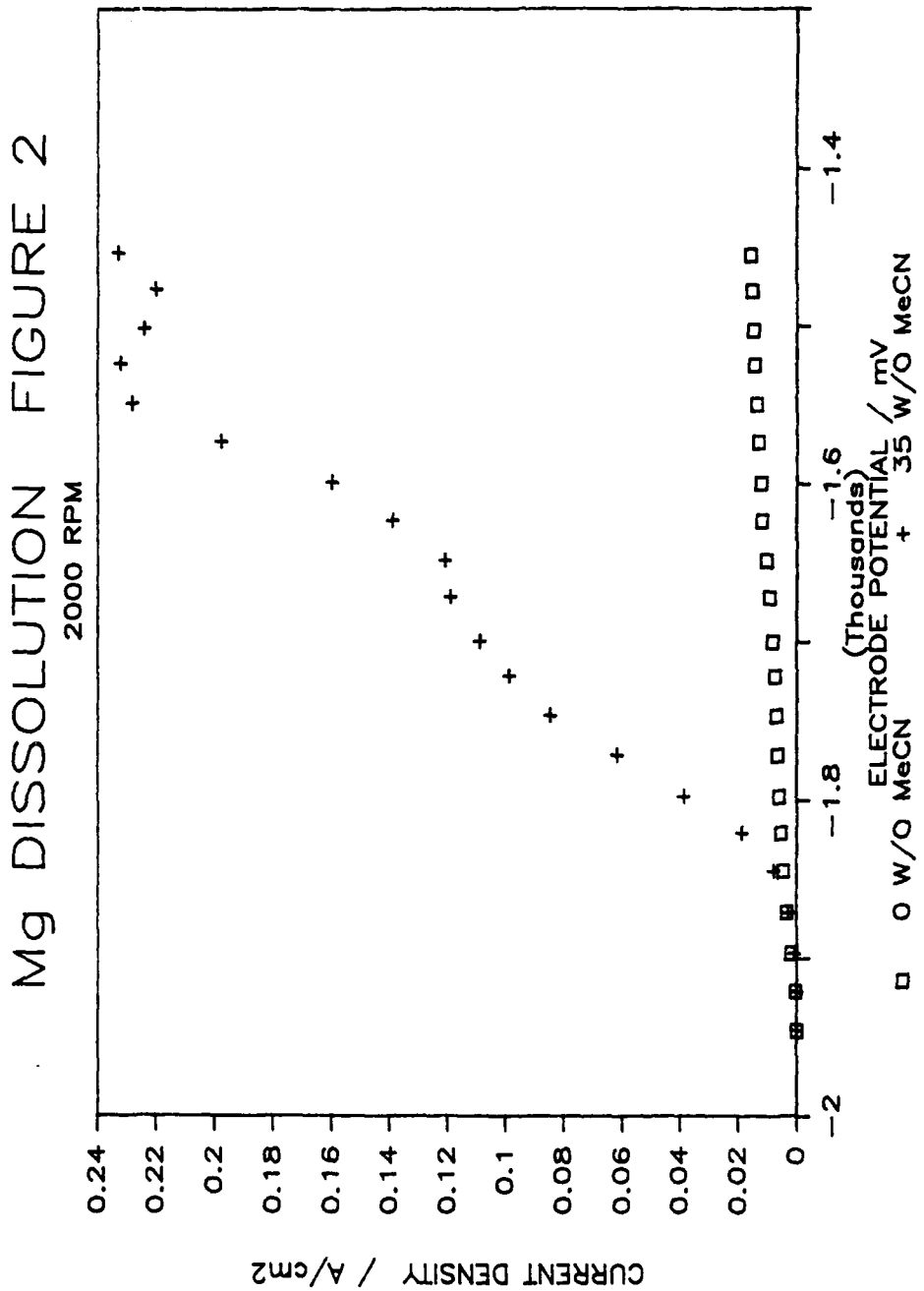
Mg DISSOLUTION FIGURE 2
2000 RPM
CURRENT DENSITY / A/cm2
0.24
0.22
0.2
0.18
0.16
0.14
0.12
0.1
0.08
0.06
0.04
0.02
0
−2
−1.8
−1.6
−1.4
(Thousands)
ELECTRODE POTENTIAL / mV
□ 0 W/O MeCN
+ 35 W/O MeCN

Section 6. Battery Studies in Low Temperature Molten Salt Electrolytes

There has been some interest in ambient temperature molten salt electrolytes for battery applications. In an early paper, the personnel at F. J. Seiler Research Laboratory tested an Al/$FeCl_3$ primary cell in a basic MEIC (1-methyl-3-ethylimidazolium chloride)-$AlCl_3$ electrolyte with benzene cosolvent (1). Subsequently, Reynolds and Dymek (2) examined primary and secondary cell configurations with MEIB (1-methyl-3-ethylimidazolium bromide)- and MEIC-AlCl3 binaries. Donahue operated continuous feed Cl_2-Al batteries in acidic and basic MEIC-$AlCl_3$ melts (3). Gifford and Palmisano tested secondary Al-Cl_2 cells based on an intercalation positive electrode which used DMPIC (1,2-dimethyl-3-propylimidazolium chloride)-$AlCl_3$ electrolytes (4). Dymek and coworkers provided data on secondary Cd-Br_2 secondary cells (5).

This paper will report on further developments of primary and secondary cells based on MEIC-$AlCl_3$ electrolytes with aluminum, magnesium, and zinc negatives and chlorine and metal halide positives. In particular, electrolytes which have been modified in various ways will be considered.

Metal-Chlorine Cells

Aluminum, magnesium, and zinc negatives were combined with chlorine positives (RVC and graphite current collectors) in basic melts (mole fraction $AlCl_3$ = 0.35) at 25°C in a cell similar to that of Donahue (3). The observed initial open circuit voltages of the cells (Al: 2.2V, Mg: 2.9V, Zn: 2.3V) were close to the calculated standard cell voltages (3) - indicating minimal self-discharge. On discharge, however, it became apparent that magnesium was undergoing significant self-discharge since its cell voltage was close to that of the aluminum and zinc at the same discharge current. The self-discharge was attributed to chlorine dissolved in the electrolyte. Aluminum negatives gave cell voltages of 1.6 and 1.3 V at currents of 10 and 20 mA, respectively (projected positive electrode area = 1.3 cm^2; negative, 7.5 cm^2) while zinc negatives gave similar results. Replacement of the MEIC with DCMEIC (1-methyl-3-ethyl-4,5-

dichloroimidazolium chloride) changed the open circuit voltage only slightly (i.e., 2.1V).

Metal - Metal Chloride Cells

Aluminum and zinc negatives were combined with copper (II) chloride and iron (III) chloride positives (RVC and graphite current collectors). Both of these positives discharge in two steps with the more positive discharge step involving a single electron transfer. For example, the reaction,

$$Al + 3\ FeCl_3 \rightarrow AlCl_3 + 3\ FeCl_2 \qquad [1],$$

has a standard cell voltage of 1.85 V while the subsequent process,

$$Al + 3/2\ FeCl_2 \rightarrow AlCl_3 + 3/2\ Fe \qquad [2],$$

has a standard cell voltage of 0.9 V. Thus, discharges will exhibit separate voltage plateaus.

The experiments were carried out in a cell like that shown in Fig. 1. The positive electrode/collector was located in the base of the cell and a small platinum foil was used to carry the current out of the glass cell wall. The projected area of the positive was 4.9 cm^2. The negative electrode was a cylinder of the metal with an stainless steel rod used to carry the current out of the cell top. The projected area of the negative was 3.8 cm^2.

In the case of the 'basic' electrolytes, the current collector was placed into the bottom of the cell and a saturated solution of the positive reactant was allowed to infiltrate the pores of collector until full (this approach was used since the metal halides were very soluble in the basic melts and, had a common electrolyte been used, self-discharge would have occurred). Unlike previous workers (1), we did not find that addition of benzene to a basic solution caused FeCl3 to be insoluble. A binary melt of the same composition as that used to prepare the saturated solution of positive reactant was carefully placed on top of the positive and the cell assembly was completed by adjusting the spacing between the electrodes and screwing the top.

The open circuit cell voltages for the basic, "duplex" (layer of binary on top of

the saturated positive reactant mixture) electrolytes ($Al/CuCl_2$: 2.1V, $Zn/CuCl_2$: 2.1V) were larger than the computed standard cell voltages. These cells were suitable for primary or reserve applications. An $Al/CuCl_2$ was discharged for twenty-one hours at 1 mA (when it was terminated at 1.2V) while another was discharged (to 0.9 V) for 8 hours at 2 mA. The second plateau voltage (on open circuit) was 1.5 V. A zinc negative cell was discharged at 1 mA for 20 hours to a voltage of 1.4 V.

It was found that the positive reactants were more-or-less insoluble in the acidic melts. Positive current collectors were impregnated with the reactant species by evacuation of a solution of the metal halide in methanol or benzene. Thus, a true common (binary) electrolyte was possible for the acidic melts. Further, it seemed possible to test the cyclability of the cells since aluminum (6) and $FeCl_3/FeCl_2$ (7) and $CuCl_2/CuCl$ (8) have been shown to be reversible in these and similar melts.

The open circuit cell voltages for the binary acidic, common electrolytes ($Al/CuCl_2$: 1.9V, $Al/FeCl_3$: 1.9V, $Zn/FeCl_3$: 1.7V) were all larger than the calculated standard cell voltages. On the other hand, open circuit cell voltages for ternary acidic (addition of benzene to lower viscosity, increase conductivity, but retain reversibility), common electrolyte cells were smaller ($Al/FeCl_3$: 1.7 V) than the calculated standard cell voltage - indicating self-discharge.

All of the acidic, binary melts were treated as secondary cells. Charge and discharge data were obtained using an IBM/PC outfitted with an IBM DACA board connected to an Amel Model 551 Galvanostat/Potentiostat operated in the galvanostatic mode. Discharges were carried out to a 0.9 V cutoff while charges were terminated at 2.09 V (to avoid evolution of chlorine in the cell). Discharge currents could be operator chosen (typically, 2.5, 5, 10, 20, 30 mA) as well as the charging current (usually, 2.5 mA). Figure 2 is an example of part of a regimen, open circuit (after a charge) - discharge (5 mA) - open circuit - charge (2.5 mA), for an $Al/FeCl_3$ cell.

Figure 3 is an example of three different discharges of the same $Al/FeCl_3$ cell at 10 mA for two different electrode spacings. Two of the discharges took place after discharge-charge cycles including discharge currents as large as 70 mA.

Although the solubility of the positive reactant species was low, the solubility of the intermediate product species (CuCl and $FeCl_2$) seemed to be greater - causing self-discharge of the negative (e.g., iron 'flakes' were found on Al electrodes which had been in discharged cells for three days or more).

References

1. D. Floreani, D. Stech, J. Wilkes, J. Williams, B. Piersma, L. King, and R. Vaughn. *Proceedings 30th Power Sources Symposium.* pp. 84-86.

2. G. F. Reynolds and C. H. Dymek. *J. Power Sources, 15*, 109 (1985).

3. F. M. Donahue. FJSRL-TM-84-002. F. J. Seiler Research Laboratory, USAF Academy, CO, 1984.

4. P. R. Gifford and J. B. Palmisano. *J. Electrochem. Soc., 135*, 650 (1988).

5. C. J. Dymek, G. F. Reynolds, and J. S. Wilkes. ibid., 134 (1987).

6. J. J. Auborn and Y. L. Barberio. *ibid., 132*, 598 (1985).

7. C. Nanjundiah, K. Shimizu, and R. A. Osteryoung. *ibid., 129*, 2474 (1982).

8. C. Nanjundiah and R. A. Osteryoung. *ibid., 130*, 1312 (1983).

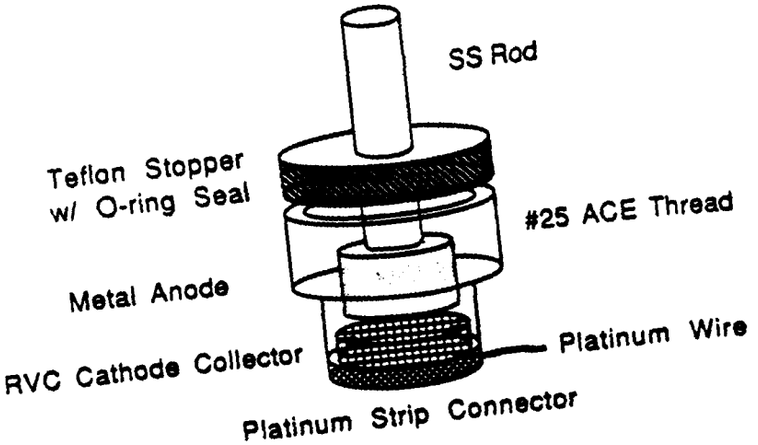

Figure 1. Sketch of Metal - Metal Chloride Cell

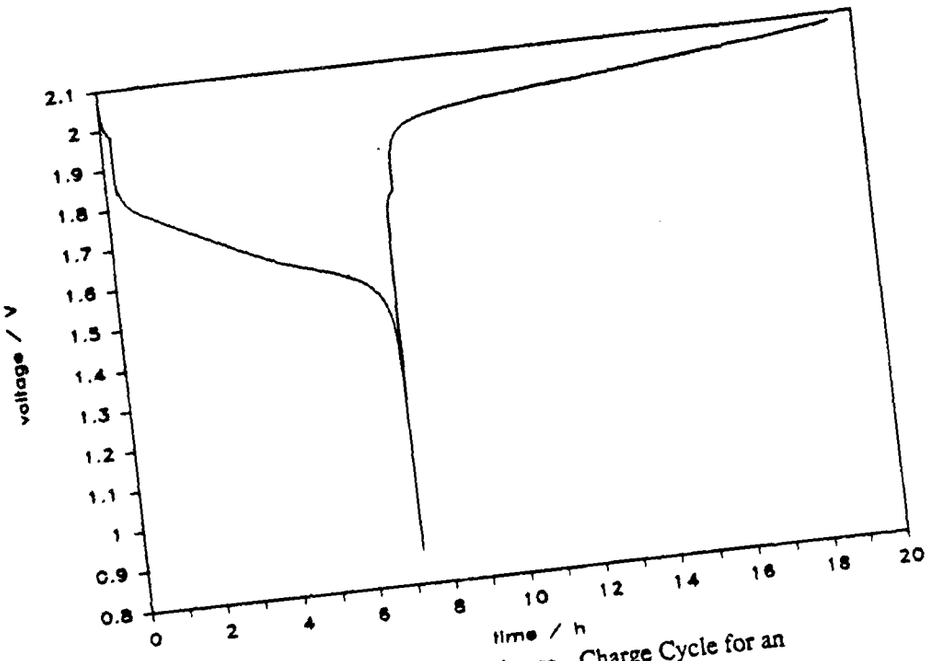

Figure 2. Part of a Discharge - Charge Cycle for an Al/$FeCl_3$ Cell.

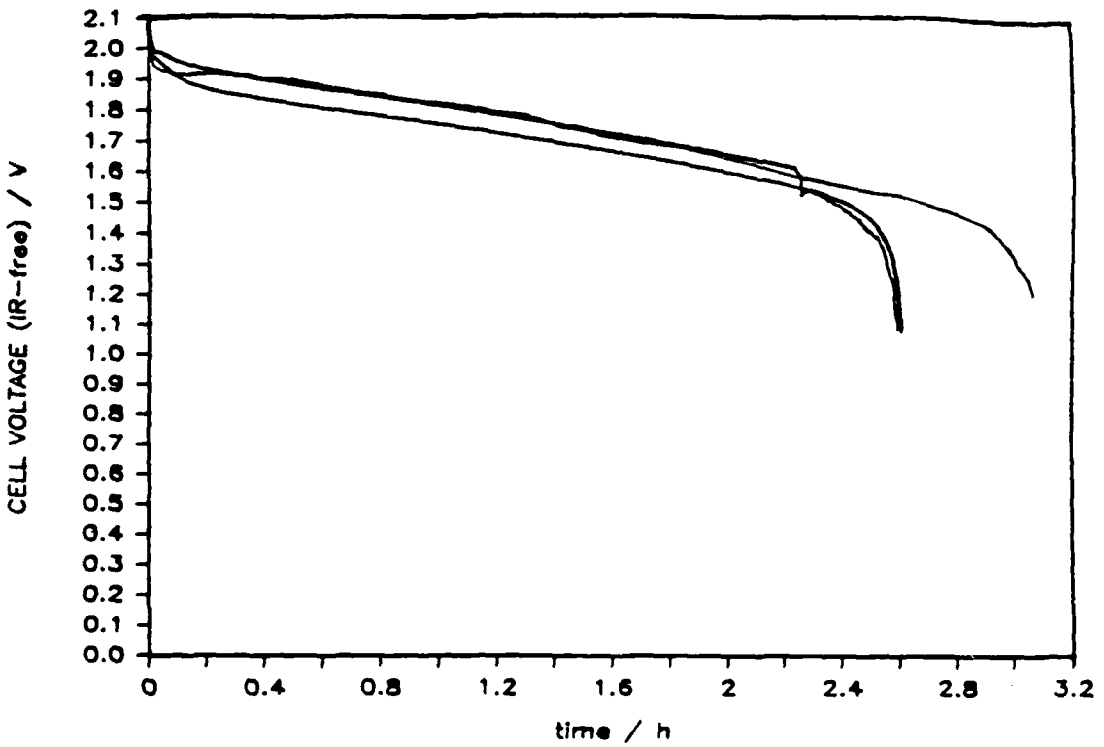

Figure 3. Discharge Curves (10 mA, IR-free) for an Al/$FeCl_3$ Cell.